Photon-exchange induces optical nonlinearities in harmonic systems

2015 J. Phys. B: At. Mol. Opt. Phys. 48 065401

(http://iopscience.iop.org/0953-4075/48/6/065401)

IOP Publishing Journal of Physics B: Atomic, Molecular and Optical Physics
J. Phys. B: At. Mol. Opt. Phys. **48** (2015) 065401 (20pp) doi:10.1088/0953-4075/48/6/065401

Photon-exchange induces optical nonlinearities in harmonic systems

Rachel Glenn, Kochise Bennett, Konstantin E Dorfman and Shaul Mukamel

Department of Chemistry, University of California, Irvine, CA 92697-2025, USA

E-mail: rglenn@msu.edu, kcbennet@uci.edu and smukamel@uci.edu

Received 21 July 2014, revised 15 October 2014
Accepted for publication 2 December 2014
Published 20 February 2015

Abstract

The response of classical or quantum harmonic oscillators coupled linearly to a classical field is strictly linear; all nonlinear response functions vanish identically. We show that, if the oscillators interact with quantum modes of the radiation field, they acquire nonlinear susceptibilities. The effective third order susceptibility $\chi^{(3)}$ induced by four interactions with quantum modes contains collective resonances involving pairs of oscillators. All nonlinearities are missed by the conventional approximate treatment based on the quantum master equations.

Keywords: harmonic, vacuum, nonlinearities

(Some figures may appear in colour only in the online journal)

1. Introduction

When a harmonic oscillator is coupled linearly to a classical field via the interaction $xE(t)$ its response is strictly linear [1]. This can easily be seen from the Heisenberg equation of motion for a damped harmonic oscillator, $\ddot{x} + \omega_0^2 x - \gamma\dot{x} = e/mE(t)$. The Fourier transform of this equation gives a linear response for any value of the field [2] $x(\omega) = \chi^{(1)}(\omega)E(\omega)$, where

$$\chi^{(1)}(\omega) = \frac{e/m}{\omega_0^2 - \omega^2 + \mathrm{i}\gamma\omega}. \tag{1}$$

For this system all higher order susceptibilities vanish identically as a result of quantum interference of different pathways of the density matrix [2, 3]. A finite nonlinear response may be induced by two mechanisms: adding anharmonicites to the potential or by incorporating a nonlinear coupling between the oscillator and the field e.g. $E(t)x^2$. In multidimensional spectroscopy, these are known as mechanical and electronic nonlinearities, respectively [4]. Nonlinear coupling to a bath [5] can also cause a nonlinear response.

Multidimensional spectroscopy of molecular vibrations with infrared pulses is widely used to study the secondary structure of proteins, hydrogen bonding in liquid water, protein folding, and chemical exchange [6–11]. These applications use an exciton Hamiltonian. In optical spectroscopy of semiconductors [12–16] and photosynthetic complexes [17], Coulomb interactions cause anharmonicities whereby Pauli exclusion affects the dipole coupling.

A Liouville-space superoperator formalism has been applied to all of the above techniques and has facilitated the analysis of complicated signals by allowing the pre-selection of relevant pathways (represented diagrammatically).

The vanishing of the nonlinear response of harmonic oscillators makes them a convenient, background-free reference system for describing the response of more complex systems. The oscillator picture is natural for intermolecular and intramolecular vibrational modes, where the oscillators represent the actual coordinates of atoms. Multidimensional spectroscopy of molecular liquids has been formulated using this model [4]. The same model applies to the optical response of many-body exciton systems such as molecular aggregates or semiconductor nanostructures [18]. In these applications the oscillators are not the actual particles (electrons), but rather collective, quasiparticle coordinates that represent electron–hole pairs. The harmonic oscillator model serves as a reference for the quasiparticle representation of the many-body response. Although it is nearly impossible to visualize the wavefunction of a many-body Fermion system, a few quasiparticles can be easily managed and calculated.

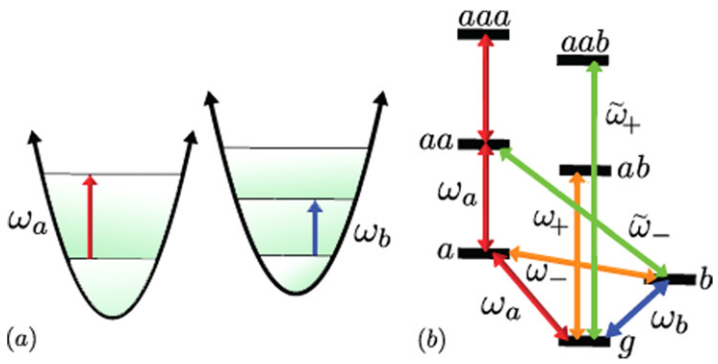

Figure 1. (a) Two uncoupled harmonic oscillators a and b with transition frequencies ω_a and ω_b. (b) The relevant level scheme for the $\chi^{(3)}$ susceptibility. The quantum mode corrections induces an effective $\chi^{(3)}$ that contains the the collective transition frequencies $\omega_\pm = \omega_a \pm \omega_b$ (yellow) and $\tilde{\omega}_\pm = 2\omega_a \pm \omega_b$ (green); as well has the single oscillator frequencies (blue and red) in the two-particle eigenstates. The exchange of oscillator a and b in the level scheme also occurs.

Here, we show that coupling to vacuum modes of the radiation field induces nonlinearities in the response of a system of harmonic oscillators, and can result in new, collective resonances. We demonstrate that coupling via the exchange of vacuum photons induces nonlinearities in the response of a system of harmonic oscillators. Photon exchange can occur either sequentially, where one oscillator emits the photon and another absorbs it, or non-sequentially, where there are interactions with the classical fields in-between. Sequential photon exchange can be described using the quantum master equation (QME) approach [19, 20]. The coupling between oscillators via photon exchange of the quantum field is then described by effective dipole–dipole and spontaneous emission (superradiance) coupling terms. In the near-field limit, the dipole–dipole coupling parameter varies as r_{ab}^{-3} with the distance between oscillators, while in the far-field limit this dependence becomes r_{ab}^{-1}. We show that systems described by the QME remain linear. This should be expected because the Hamiltonian is quadratic in the boson creation and annihilation operators. However, a more general diagrammatic expansion of the signal generates terms with non-sequential photon exchange with a field correlation function of the vacuum modes which is quartic in the boson creation and annihilation operators. This induces a finite nonlinear response. Four-wave mixing (FWM) of classical and quantum fields coupled to two harmonic oscillators a and b, has both single-oscillator and collective resonances. Figure 1(a) shows two uncoupled harmonic oscillators and (b) shows the level-scheme with the single and collective transition frequencies involved in the induced nonlinear response.

The nonlinear response of a system of N non-interacting oscillators is N times the single oscillator response, which vanishes in the harmonic case. To second order, coupling to the vacuum modes of the electromagnetic field results in a susceptibility that is given by a sum of a product of individual susceptibilities. For instance, in [21] we showed that the coupling of the quantum modes to first-order for a system composed of particles i and j can create a fifth-order susceptibility $\chi^{(5)}$ which is the product of two susceptibilities $\chi^{(5)} = \chi_i^{(3)}\chi_j^{(3)}$. We showed that these non-additive contributions can induce collective resonances that only arise in a quantum field framework and, in [22], such resonances were predicted for two level chromophores. Corrections to harmonic systems come at higher order in the vacuum-mode coupling.

The first-order correction to the nonlinear response is proportional to two interactions with the quantum fields, which are initially in the vacuum state. This contribution is proportional to the semi-classical single-oscillator $\chi^{(3)}$, which vanishes for our model. It is well known that a Hamiltonian which is quadratic in the boson creation and annihilation operators can be diagonalized and thus there should be no nonlinear effects; these require an anharmonicity. For our model, the lowest-order finite nonlinear response is fourth order in the quantum fields. Using Wick's theorem this correlation function can be written as a product of two quadratic field correlation functions. The effective $\chi^{(3)}$, caused by interaction with four quantum modes. $\chi^{(3)}$ has two contributions. The first is the product of $\chi_a^{(3)}$ from oscillator a and $\chi_b^{(3)}$ from oscillator b and represents a resonant energy transfer, where each oscillator interacts twice with the quantum modes. We find that the quartic quantum field correlation function vanishes for this contribution. The second contribution to the susceptibility is of the form $\chi_a^{(5)}\chi_b^{(1)}$, which involves both a cascading process [21], where oscillator b emits a photon and oscillator a absorbs it, and a process where oscillator a emits and absorbs the same photon. The latter is typically neglected when calculating the resonant energy transfer between molecules [27]. We show that this term may not be neglected when considering harmonic oscillators, since it is responsible for the finite nonlinear response. The time-ordered $\chi_a^{(5)}$ correlation function contains two dipole-operators associated with emission and absorption of a single photon with oscillator a, which cannot be factorized out to renormalize the nonlinear response function.

Note that the oscillator picture can represent the collective excitations of a complicated system composed of many particles (e.g. electrons). The process where oscillator a emits and absorbs a photon is analogous to similar processes that occur on the level of the constituent particles and are interpreted as renormalizing their bare properties (mass and charge). These latter processes are therefore implicitly included in the oscillator properties but differ from the renormalization of the collective excitations of this many-particle system (modeled by the harmonic oscillator levels) that we consider in this paper. On a microscopic level, this can represent the emission by one constituent particles and absorption by another. Such processes originate in intramolecular self-energy terms which are normally neglected in molecular quantum electrodynamics [27].

This paper is organized as follows. In section 2, we present the model of the system and its response in a compact formal expression that contains all orders in the fields and serves as a starting point for perturbative calculations of the corrections to various signals due to quantum modes of the radiation field. In section 3, we calculate the correction to the linear absorption spectrum from coupling to the quantum field modes. In section 4, we demonstrate that this coupling leads to a finite third-order nonlinear response and in section 5, we present the FWM signal obtained with continuous wave (cw) lasers. For comparison, the response calculated using the QME is presented in section 6. The results are discussed in section 7.

2. Model and the nonlinear response

We consider a system of uncoupled harmonic oscillators which interact with the radiation field and described by the Hamiltonian

$$H = H_0 + H_{\text{int}}, \tag{2}$$

where

$$H_0 = \sum_\alpha \omega_\alpha B_\alpha^\dagger B_\alpha \tag{3}$$

is the oscillator Hamiltonian and $B_\alpha^\dagger$ (B_α) is the boson creation (annihilation) operator of the αth oscillator which satisfy the commutation $[B_\alpha, B_\beta^\dagger] = \delta_{\alpha\beta}$.

The radiation field is given as

$$E(\mathbf{r}, t) = E^0(\mathbf{r}, t) + E^\nu(\mathbf{r}, t), \tag{4}$$

where $E^0(\mathbf{r}, t) = \mathcal{E}_0(\mathbf{r}, t) + \mathcal{E}_0^*(\mathbf{r}, t)$ is a classical incoming field and the second term represents the quantum vacuum modes $E^\nu(\mathbf{r}, t) = \mathcal{E}_\nu(\mathbf{r}, t) + \mathcal{E}_\nu^\dagger(\mathbf{r}, t)$

$$\mathcal{E}_\nu(\mathbf{r}, t) = \sum_{\mathbf{k}_\nu, \lambda} \left(\frac{2\pi c \omega_\nu}{\mathcal{V}}\right)^{1/2} \epsilon^{(\lambda)}(\mathbf{k}_\nu) a_{\mathbf{k}_\nu,\lambda} \mathrm{e}^{-\mathrm{i}\omega_\nu t + \mathrm{i}\mathbf{k}_\nu \cdot \mathbf{r}}. \tag{5}$$

$\mathcal{V}$ denotes the quantization volume, $\epsilon^{(\lambda)}$ is the polarization vector for mode $\mathbf{k}_\nu$ and λ is the polarization. $a_{\mathbf{k}_\nu,\lambda}$ is the Boson annihilation operator. The matter–field interaction, in the interaction picture, with respect to the Hamiltonian, H_0 is

$$H_{\text{int}} = -\sum_\alpha E(t, \mathbf{r})\Big(V_\alpha(t) + V_\alpha^\dagger(t)\Big). \tag{6}$$

$V_\alpha(t) = \mu_\alpha B_\alpha(t)$ is the dipole coupling and μ_α is the transition dipole matrix element. To simplify the expression in equation (6) we do not invoke the rotating-wave-approximation.

The optical response will be calculated using superoperator algebra [23] for the density matrix in Liouville space. The frequency dispersed response to the electric field is given by [2]

$$S(\omega) = -\mathcal{I}\Bigg[\mathcal{E}_0^*(\omega, \mathbf{r}) \int_{-\infty}^{\infty} \mathrm{d}t \times \left\langle V_L(t) \mathrm{e}^{-\frac{\mathrm{i}}{\hbar}\int_{-\infty}^{t} H_{\text{int}-}(T)\mathrm{d}T} \right\rangle \mathrm{e}^{\mathrm{i}\omega t}\Bigg], \tag{7}$$

where $\mathcal{I}$ denotes the imaginary part. Equation (7) will be perturbatively expanded in the field–matter interaction to calculate the correction to the linear and nonlinear response functions due to vacuum mode coupling. We define the linear combinations of superoperators

$$O_- = O_{\text{L}} - O_{\text{R}} \tag{8}$$

and

$$O_+ = \frac{1}{2}\big(O_{\text{L}} + O_{\text{R}}\big), \tag{9}$$

where the two superoperators O_{L} and O_{R} are defined by their actions from the left $O_{\text{L}}X \leftrightarrow OX$ and from the right $O_{\text{R}}X \leftrightarrow XO$ [23].

3. Photon exchange correction to the linear response $\chi^{(1)}$

The diagrammatic expansion of equation (7) to first-order in H_{int}, with the classical fields, is presented in figure 2(a). In these diagrams we work in the ± representation. Time progresses as one moves up the diagrams and the vertical lines represent the density matrices of the different molecules a and b. This provides a formal book keeping tool for the various contributions to the signal [21].

The superoperator corresponding to the interaction Hamiltonian is $(EV)_- = E_-V_+ + E_+V_-$. Because the classical fields are c-numbers, i.e. $E_- = 0$ the dipole operators associated with classical fields are V_-. The first-order expansion (figure 2(a)) for two uncoupled harmonic oscillators a and b,

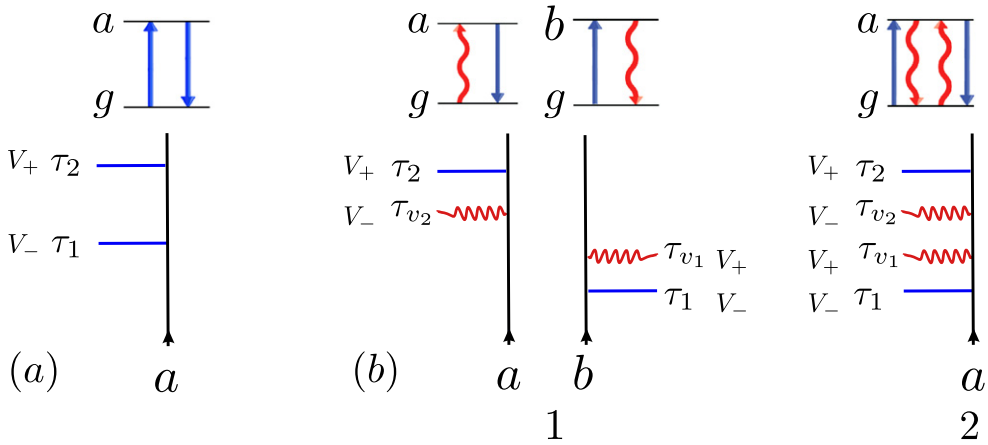

Figure 2. (a) Diagram for the linear absorption spectrum equation (10) ($\chi^{(1)}$), for a harmonic oscillator. (b) Diagrams for the nonlinear correction to the linear signal equation (10). Lines corresponding to interaction with a classical field are solid blue and with a quantum field are wavy red. The corresponding level schemes are shown above. For diagram rules see [21].

gives the classical linear response [2]

$$S^{(1)}(\omega) = \left|\mathcal{E}_0(\omega)\right|^2 \mathcal{I}\chi_0^{(1)}(-\omega;\,\omega), \tag{10}$$

where the susceptibility is given as

$$\chi_0^{(1)}(-\omega;\,\omega) = -\frac{1}{\hbar^2}\left(\frac{\left|\mu_a\right|^2}{\omega - \omega_a + \mathrm{i}\Gamma_a}\right) + a \Leftrightarrow b, \tag{11}$$

where $a \Leftrightarrow b$ represents the interchange of oscillators a and b. Equation (10) describes the process where oscillator a absorbs and emits the classical field ω. See the corresponding level scheme diagrams, figure 2(a).

The leading correction due to the vacuum modes is second-order: emission followed by absorption. We expand equation (7) to third-order in figure 2(b), (two interactions with the quantum modes and one with the classical mode). The last interaction, at time τ_2, is with a classical field ($\mathcal{E}_0^*(\omega,\,r)$ equation (7)) acting on oscillator a. Diagram 2(b)1 depicts oscillator b absorbing a photon at τ_1 from the classical field. That photon is converted into a single photon that interacts with the vacuum electromagnetic field at τ_{v_1} and propagates to oscillator a where it is absorbed at τ_{v_2}. Finally, oscillator a generates the detected signal at τ_2. See the level scheme diagram shown above figure 2(b)1. Because $\mathrm{Tr}\,[\hat{O}_-\rho] = 0$, the last interaction with the quantum mode must be E_+ (i.e., $\langle E_+E_\pm\rangle$). Similarly, the interaction at τ_{v_1} must be a quantum mode, since $\langle V_-V_-\rangle_b$ vanishes. As a result, the quantum field correlation function will be $\langle E_+E_-\rangle$. In figure 2(b)1 we label the dipole operator associated with each interaction with the field.

The effective coupling between the two oscillators depends on their distance in space and their dipole moments. We assume that the angle of the dipole moments are fixed. Figure 3 illustrates the configuration of the dipole moments $\vec{\mu}_a$ and $\vec{\mu}_b$. The emission and absorption of a single photon by oscillator a mediated by the vacuum is shown in figure 2(b)2. See the corresponding level scheme diagram above the ladder diagram.

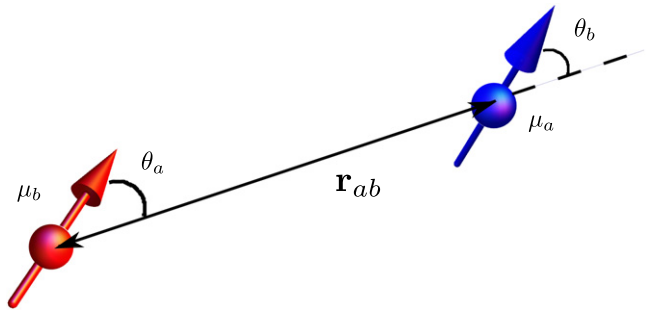

Figure 3. The dipole moments μ_a and μ_b in configuration for two oscillators separated by the distance $\mathbf{r}_{ab}$.

The signal is calculated in appendix A. Combining the absorption spectrum with the second-order vacuum mode correction gives the effective linear susceptibility

$$\chi^{(1)}(-\omega;\,\omega) = \chi_0^{(1)}(-\omega;\,\omega) + \chi_1^{(1)}(-\omega;\,\omega). \tag{12}$$

The susceptibility $\chi_0^{(1)}$ is given by equation (11) and the correction due to the interaction with the quantum modes reads

$$\begin{aligned}\chi_1^{(1)}(-\omega;\,\omega) = &-\frac{1}{\hbar^2}\left(\frac{\mu_a\mu_b^*}{\omega - \omega_a + \mathrm{i}\Gamma_a}\right)\\ &\times\frac{J_{ab}(r_{ab};\,\omega) + \mathrm{i}\gamma_{ab}(r_{ab};\,\omega)}{\hbar\left(\omega - \omega_b + \mathrm{i}\Gamma_b\right)}\mathrm{e}^{\mathrm{i}k_0 r_{ab}}\\ &-\frac{1}{\hbar^2}\left(\frac{\left|\mu_a\right|^2}{\omega - \omega_a + \mathrm{i}\Gamma_a}\right)\frac{\omega^3}{2\pi\epsilon_0 c^3}\\ &\times\frac{1}{\hbar\left(\omega - \omega_a + \mathrm{i}\Gamma_a\right)} + a \Leftrightarrow b.\end{aligned} \tag{13}$$

Here $\frac{\omega^3}{2\pi\epsilon_0 c^3}$ is proportional to the spontaneous decay, and originates from diagram 2(b)2, The effective dipole–dipole

coupling between oscillators is

$$J_{ab}(r_{ab};\,\omega) = -\frac{\mu_a^*\mu_b\omega^3}{4\pi\epsilon_0 c^3}\left[\sin\theta_a\sin\theta_b\frac{\cos(y_{ab})}{(y_{ab})} - \cos(\theta_a+\theta_b)\left[\frac{\sin(y_{ab})}{(y_{ab})^2} + \frac{\cos(y_{ab})}{(y_{ab})^3}\right]\right] \quad (14)$$

and the effective cooperative emission [19] is

$$\gamma_{ab}(r_{ab};\,\omega) = \frac{\mu_a^*\mu_b\omega^3}{4\pi\epsilon_0 c^3}\left[\sin\theta_a\sin\theta_b\frac{\sin(y_{ab})}{(y_{ab})} + \cos(\theta_a+\theta_b)\left[\frac{\cos(y_{ab})}{(y_{ab})^2} - \frac{\sin(y_{ab})}{(y_{ab})^3}\right]\right], \quad (15)$$

where $y_{ab} \equiv \omega r_{ab}/c$.

The dipole–dipole and spontaneous emission contributions originate from the process depicted in diagram 2(b)1. For the dipole–dipole coupling in the near zone, $y_{ab} \ll 1$, the second term in the square brackets of equation (14) becomes dominant and the susceptibility scales as r_{ab}^{-3}, which is recognizable as the static dipole–dipole coupling. For the far field limit, $y_{ab} \gg 1$, the first term in equation (14) becomes dominant and the susceptibility depends the separation distance as r_{ab}^{-1}.

The linear absorption spectrum, equation (10),

$$S_0^{(1)}(\omega_3) = -\mathcal{I}\chi_0^{(1)}(-\omega_3;\,\omega_3), \quad (16)$$

where the effective susceptibility is given by equation (11). Equation (16) is plotted in figure 4(a) using a red-dashed line.

The linear signal that includes the correction from the quantum field is given by

$$S^{(1)}(\omega_3) = -\mathcal{I}\chi^{(1)}(-\omega_3;\,\omega_3). \quad (17)$$

with $\chi^{(1)}(-\omega_3;\,\omega_3)$ given by equation (12). The correction $S^{(1)}(\omega_3)$ is plotted in figure 4(a) using a solid-blue line. The absorption spectrum (dashed-red) shows two absorption peaks at $\omega_3 = \omega_a,\ \omega_b$. The correction from the quantum modes (solid-blue line) in figure 4(a) changes the absorption peak at $\omega_3 = \omega_b$ to have both absorption and emission features. As r_{ab} increases, ($r_{ab}/2\pi\lambda_a = 0.2$ in figure 4(b)), the correction from the quantum modes weakens and $\chi_1^{(1)}$ approaches $\chi_0^{(1)}$.

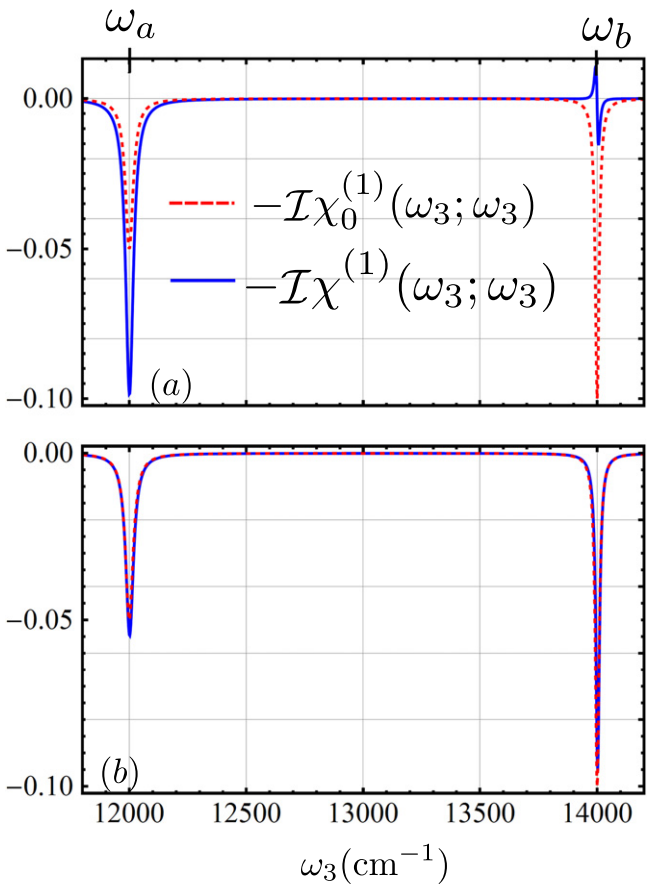

Figure 4. The absorption spectrum for a cw laser (dashed-red) of two harmonic oscillators a and b and the correction the linear response from the quantum modes equation (12) (solid-blue) are plotted in the units $\frac{1}{\hbar^2}|\mu_a|^2$. The distance between oscillators is (a) $r_{ab}/2\pi\lambda_a = 0.09$ and (b) $r_{ab}/2\pi\lambda_a = 0.2$. The oscillator frequencies used are $\omega_a = 12\,000\ \mathrm{cm}^{-1}$, $\omega_b = 14\,000\ \mathrm{cm}^{-1}$ and the decay rates are $\Gamma_a = n\tilde{\Gamma}_a$ and $\Gamma_b = m\tilde{\Gamma}_b$, where n and m are the excitation level of the oscillator, $\tilde{\Gamma}_a = 20\ \mathrm{cm}^{-1}$ and $\tilde{\Gamma}_b = 10\ \mathrm{cm}^{-1}$. The dipole moments are in the units $\mu_{na,a} = \sqrt{n}\mu_a$, $\mu_b = 0.99\sqrt{m}\mu_a$.

4. $\chi^{(3)}$ nonlinearity induced by photon-exchange

The third-order susceptibility vanishes for harmonic oscillators when coupling to the quantum vacuum modes is neglected. The lowest-order possible correction is second-order in the quantum modes, which are initially in the vacuum state. This contribution vanishes as well, as can be understood from the diagrammatic expansion of equation (7) to fifth order in H_{int}. See figure 5. This process is third-order in the classical fields and second-order the quantum fields. In this process, oscillator b absorbs a photon from the classical field at τ_1 and emits a vacuum photon at τ_{v_1}, which then propagates to oscillator a where it is absorbed at τ_{v_2}. Oscillator a interacts with the classical field at τ_2 and τ_3 and generates the detected signal at τ_4. These diagrams offer a compact representation of the signal generation. Because the susceptibility can written as $\chi_{ab}^{(5)} = \chi_b^{(1)}\chi_a^{(3)}$, there will be eight possible quantum pathways for oscillator a and one for oscillator b. Overall, the third-order process contains three classical field interactions and be viewed as an effective $\chi^{(3)}$. For the vacuum trace to be finite, the final interaction with a quantum mode on oscillator a must be E_+V_- and the quantum mode interaction on oscillator b must be E_-V_+. From figure 5, the matter correlation function for oscillator a will have form $\langle V_+V_-V_-V_-\rangle_a$ and oscillator b will have the form $\langle V_+V_-\rangle_b$. The semiclassical response $\langle V_+V_-V_-V_-\rangle$ is zero for the harmonic system. Since the Hamiltonian equation (3) is quadratic in the boson creation and annihilation operators, the nonlinear response vanishes when coupling to the quantum modes is neglected. When the interaction Hamiltonian equation (6) is expanded to

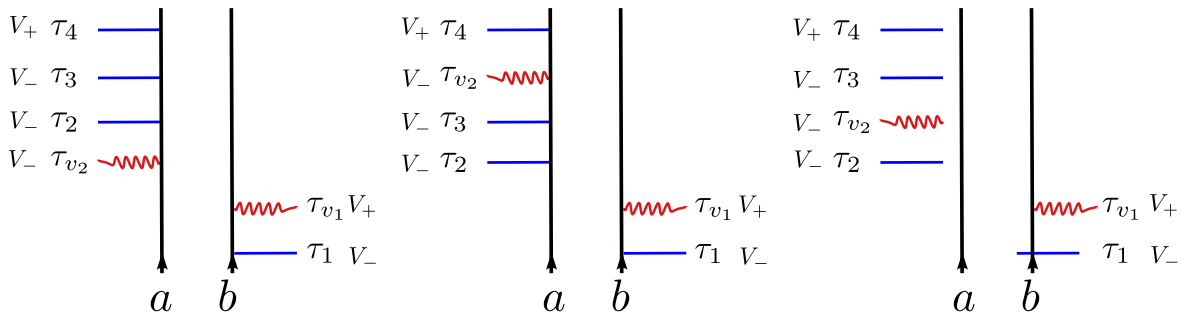

Figure 5. The nonlinear response equation (7) for two uncoupled harmonic oscillators expanded to fifth order, two interactions with the quantum modes (wavy red) and four interactions with the classical modes (solid blue).

quadratic order in the quantum vacuum modes, the correction vanishes and harmonic oscillator remains linear. Obtaining a non-vanishing correction will require us to expand the signal equation (7) to higher order in the quantum modes.

The next order correction to the nonlinear response is fourth-order. For two harmonic oscillators a and b, the signal can be separated into two contributions. The first is where oscillators a and b both interact twice with the quantum modes. This contribution to the signal is 7th order in H_{int} and shown in figure 6. The permutations of the quantum field modes in the diagram of figure 6 will give a total of 14 diagrams, which are not shown here. This can describe the process where oscillator b interacts with the classical fields at τ_1, τ_2, and then interacts with the vacuum electromagnetic field to emit a photon at τ_{v_1}, and absorb a photon at τ_{v_2}. Oscillator a absorbs a photon at τ_{v_3}, and emits a photon at τ_{v_4} via the vacuum. Then oscillator a interacts with the classical field at τ_3 and generates the detected field at τ_4. Similar processes will also occur due to the permutations of the quantum and classical fields. The associated susceptibility $\chi_{ab}^{(5)}$ can be factorized as $\chi_a^{(3)}\chi_b^{(3)}$. Similar to the diagrams with two quantum modes (figures 2, 5) the last quantum mode on oscillator a at time τ_{v_4} in the diagram 6 has a V_- associated with it. The first quantum mode on oscillator a at time τ_{v_3} can be $V_\pm$. However, since $\langle V_+V_-V_-V_-\rangle_a$ vanishes for the harmonic oscillator, the interaction at time τ_{v_3} must be V_+. For oscillator b, the last quantum mode at τ_{v_2} is V_+. Because $\langle V_+V_-V_-V_-\rangle_b$ vanishes, this requires the first quantum mode at τ_{v_1} to be V_+. The diagram in figure 6, will acquire a quantum field correlation function of form $\langle E_+E_-E_-E_-\rangle$, which vanishes for the bosonic fields. This means that there is no resonant energy transfer between two harmonic oscillators.

The second contribution yields a finite nonlinear signal and involves three quantum modes interacting with oscillator a and one quantum mode interacting with oscillator b and vise versa. See figure 7 for the diagrammatic expansion. This contribution can describe the process where oscillator b absorbs a photon from the field at τ_1. Oscillator b then emits a photon at τ_{v_1} and that propagates to oscillator a where it is absorbed at τ_{v_2}. Oscillator a emits and absorbs a photon with the vacuum electromagnetic field at τ_{v_3} and τ_{v_4}. Finally, oscillator a interacts with the field at times τ_{v_2} and τ_{v_4} to

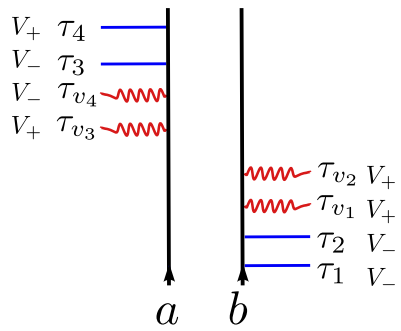

Figure 6. Diagram for the nonlinear response equation (7) expanded to seventh order, four interactions with the quantum modes (wavy red) and four interactions with the classical modes (solid blue) for two uncoupled harmonic oscillators. These diagrams can represent resonant energy transfer between harmonic oscillators.

generate the signal. The nonlinear response will include all permutations of the quantum and classical field modes, which will describe a similar processes. The resulting susceptibility is $\chi_{ab}^{(5)} = \chi_a^{(5)}\chi_b^{(1)}$, which is an effective $\chi^{(3)}$, since it is third order in external fields.

Derivation of the heterodyne signal for the diagram in figure 7 is given in appendix B. Equation (B18) gives the effective third-order susceptibility

$$\begin{aligned}
&\chi^{(3)}(-\omega;\,\omega_1,\,\omega_2,\,\omega_3)\\
&\quad=\left(\frac{1}{2\pi\hbar}\right)^8\int \mathrm{d}\omega_{v_1}\mathrm{d}\omega_{v_2}\tilde{D}_{aa}^{(\mu,\mu')}(\omega_{v_1})\\
&\qquad\times\frac{\hbar}{\mu_a\mu_b}\Big[J_{ab}\big(r_{ab};\,\omega_{v_2}\big)-\mathrm{i}\gamma_{ab}\big(r_{ab};\,\omega_{v_2}\big)\Big]\\
&\qquad\times\Big\{\chi_{+-----+}^{\nu_1\nu_2,\nu_2}(\omega,\,\omega_{\nu_1},\,\omega_3,\,\omega_{\nu_2},\,\omega_2,\,\omega_{\nu_2})\\
&\qquad+\chi_{+---+-}^{\nu_1\nu_2,\nu_2}(\omega,\,\omega_3,\,\omega_2,\,\omega_{\nu_1},\,\omega_{\nu_2},\,\omega_{\nu_2})\\
&\qquad+\chi_{+--+--}^{\nu_1\nu_2,\nu_2}(\omega,\,\omega_{\nu_1},\,\omega_{\nu_2},\,\omega_{\nu_2},\,\omega_3,\,\omega_2)\\
&\qquad+\chi_{+--+--}^{\nu_2\nu_2,\nu_1}(\omega,\,\omega_{\nu_2},\,\omega_{\nu_2},\,\omega_{\nu_1},\,\omega_3,\,\omega_2)\\
&\qquad+\chi_{+---+-}^{\nu_2\nu_2,\nu_1}(\omega,\,\omega_3,\,\omega_2,\,\omega_{\nu_2},\,\omega_{\nu_2},\,\omega_{\nu_1})\\
&\qquad+\chi_{+-+---}^{\nu_2\nu_2,\nu_1}(\omega,\,\omega_{\nu_2},\,\omega_3,\,\omega_{\nu_2},\,\omega_{\nu_1},\,\omega_2)\Big\}\\
&\qquad+a\Leftrightarrow b,
\end{aligned}\tag{18}$$

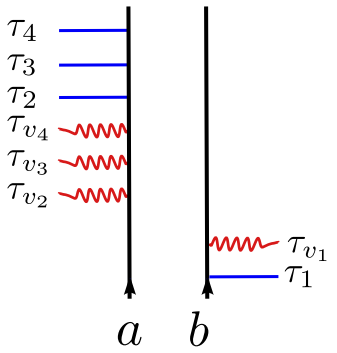

Figure 7. Diagrammatic expansion of equation (7) to seventh-order in $H_{\rm int}$. The diagram contains four interactions with the quantum modes and four interactions with the classical field modes. This contribution gives rise to an effective third-order susceptibility.

where $\tilde{D}_{aa}^{(\mu,\mu')}(\omega_{\nu_1})$ is given by equation (A6) and the dipole–dipole and spontaneous emission coupling term are given by equations (14), (15), respectively. In equation (18), the susceptibility $\chi_{+--+--}^{\nu_2\nu_2,\nu_1}$ appears twice to account for the two permutations of the quantum mode coupling. The superscript $\nu_i\nu_j$, ν_k corresponds to the designation of the quantum modes at times τ_{ν_4}, τ_{ν_3} and τ_{ν_2}, respectively. For example, the index $\nu_2\nu_2$, ν_1 corresponds to ω_{ν_1} at time τ_{ν_2} and ω_{ν_2} at τ_{ν_3} and τ_{ν_4}. If ω_{ν_2} is positive at τ_{ν_3} then it will be negative at time τ_{ν_4}, and vise versa. This is because it must emit and absorb the the same quantum mode ω_{ν_2}. Here

$$\begin{aligned}
&\chi_{+----+}^{\nu_1\nu_2,\nu_2}(\omega,\omega_{\nu_1},\omega_3,\omega_{\nu_2},\omega_2,\omega_{\nu_2})\\
&\quad=\int \mathrm{d}\tau_4\mathrm{d}\tau_3\mathrm{d}\tau_2\mathrm{d}\tau_1\\
&\qquad\times\int \mathrm{d}\tau_{\nu_4}\mathrm{d}\tau_{\nu_3}\mathrm{d}\tau_{\nu_2}\mathrm{d}\tau_{\nu_2}\theta(\tau_{\nu_2}-\tau_{\nu_1})\\
&\qquad\times\Delta_{+----+}^{\nu_1\nu_2,\nu_2}(\tau_4,\tau_{\nu_4},\tau_3,\tau_{\nu_3},\tau_2,\tau_{\nu_2})\alpha_{+-}^{\nu_1}(\tau_{\nu_1},\tau_1)\\
&\qquad\times \mathrm{e}^{-\mathrm{i}\omega\tau_4+\mathrm{i}\omega_{\nu_1}\tau_{\nu_4}+\mathrm{i}\omega_3\tau_3+\mathrm{i}\omega_{\nu_2}\tau_{\nu_3}+\mathrm{i}\omega_2\tau_2-\mathrm{i}\omega_{\nu_2}\tau_{\nu_2}},
\end{aligned}\tag{19}$$

$$\begin{aligned}
&\chi_{+---+-}^{\nu_1\nu_2,\nu_2}(\omega,\omega_3,\omega_2,\omega_{\nu_1},\omega_{\nu_2},\omega_{\nu_2})\\
&\quad=\int \mathrm{d}\tau_4\mathrm{d}\tau_3\mathrm{d}\tau_2\mathrm{d}\tau_1\\
&\qquad\times\int \mathrm{d}\tau_{\nu_4}\mathrm{d}\tau_{\nu_3}\mathrm{d}\tau_{\nu_2}\mathrm{d}\tau_{\nu_2}\theta(\tau_{\nu_2}-\tau_{\nu_1})\\
&\qquad\times\Delta_{+---+-}^{\nu_1\nu_2,\nu_2}(\tau_4,\tau_3,\tau_2,\tau_{\nu_4},\tau_{\nu_3},\tau_{\nu_2})\alpha_{+-}^{\nu_1}(\tau_{\nu_1},\tau_1)\\
&\qquad\times \mathrm{e}^{-\mathrm{i}\omega\tau_4+\mathrm{i}\omega_{\nu_1}\tau_{\nu_4}+\mathrm{i}\omega_3\tau_3+\mathrm{i}\omega_{\nu_2}\tau_{\nu_3}+\mathrm{i}\omega_2\tau_2-\mathrm{i}\omega_{\nu_2}\tau_{\nu_2}},
\end{aligned}\tag{20}$$

$$\begin{aligned}
&\chi_{+--+--}^{\nu_1\nu_2,\nu_2}(\omega,\omega_{\nu_1},\omega_{\nu_2},\omega_{\nu_2},\omega_3,\omega_2)\\
&\quad=\int \mathrm{d}\tau_4\mathrm{d}\tau_3\mathrm{d}\tau_2\mathrm{d}\tau_1\\
&\qquad\times\int \mathrm{d}\tau_{\nu_4}\mathrm{d}\tau_{\nu_3}\mathrm{d}\tau_{\nu_2}\mathrm{d}\tau_{\nu_2}\theta(\tau_{\nu_2}-\tau_{\nu_1})\\
&\qquad\times\Delta_{+--+--}^{\nu_1\nu_2,\nu_2}(\tau_4,\tau_{\nu_4},\tau_{\nu_3},\tau_{\nu_2},\tau_3,\tau_2)\alpha_{+-}^{\nu_1}(\tau_{\nu_1},\tau_1)\\
&\qquad\times \mathrm{e}^{-\mathrm{i}\omega\tau_4+\mathrm{i}\omega_{\nu_1}\tau_{\nu_4}+\mathrm{i}\omega_3\tau_3+\mathrm{i}\omega_{\nu_2}\tau_{\nu_3}+\mathrm{i}\omega_2\tau_2-\mathrm{i}\omega_{\nu_2}\tau_{\nu_2}},
\end{aligned}\tag{21}$$

$$\begin{aligned}
&\chi_{+-+---}^{\nu_2\nu_2,\nu_1}(\omega,\omega_{\nu_2},\omega_3,\omega_{\nu_2},\omega_{\nu_1},\omega_2)\\
&\quad=\int \mathrm{d}\tau_4\mathrm{d}\tau_3\mathrm{d}\tau_2\mathrm{d}\tau_1\\
&\qquad\times\int \mathrm{d}\tau_{\nu_4}\mathrm{d}\tau_{\nu_3}\mathrm{d}\tau_{\nu_2}\mathrm{d}\tau_{\nu_2}\theta(\tau_{\nu_2}-\tau_{\nu_1})\\
&\qquad\times\Delta_{+-+---}^{\nu_2\nu_2,\nu_1}(\tau_4,\tau_{\nu_4},\tau_3,\tau_{\nu_3},\tau_{\nu_2},\tau_2)\alpha_{+-}^{\nu_1}(\tau_{\nu_1},\tau_1)\\
&\qquad\times \mathrm{e}^{-\mathrm{i}\omega\tau_4+\mathrm{i}\omega_{\nu_2}\tau_{\nu_4}+\mathrm{i}\omega_3\tau_3-\mathrm{i}\omega_{\nu_2}\tau_{\nu_3}+\mathrm{i}\omega_2\tau_2+\mathrm{i}\omega_{\nu_1}\tau_{\nu_2}}.
\end{aligned}\tag{22}$$

The fifth-order susceptibility Δ for oscillator a is defined as

$$\begin{aligned}
&\Delta_{+-\zeta_1\zeta_2\zeta_3\zeta_4}^{\nu_4\nu_3,\nu_2}(\tau_4,\tau_{\nu_4},\tau_3,\tau_{\nu_3},\tau_2,\tau_{\nu_2})\\
&\quad=\left\langle \mathcal{T}\ V_L(\tau_4)V_-^{\nu_4}(\tau_{\nu_4})V_{\zeta_1}(\tau_3)V_{\zeta_2}^{\nu_3}(\tau_{\nu_3})V_{\zeta_3}(\tau_2)V_{\zeta_4}^{\nu_2}(\tau_{\nu_2})\right\rangle_a,
\end{aligned}\tag{23}$$

where ζ_i can be $\pm$. The first-order susceptibility α from oscillator b is

$$\alpha_{+-}^{\nu_1}(\tau_{\nu_1},\tau_1)=\left\langle \mathcal{T}V_+^{\nu_1}(\tau_{\nu_1})V_-(\tau_1)\right\rangle_b.\tag{24}$$

The two frequency integrations in equation (18) over ω_{ν_1} and ω_{ν_2} may be done analytically using contour integration. Note that the frequencies ω_1, ω_2 and ω_3 in the susceptibility (18) can be positive or negative. The integration over τ_4 in equations (19)–(22) will give a delta function, which originates from time translational invariance that can be used to evaluate the ω_3 integration in equation (B18). This leaves the integrations over ω_1 and ω_2 in equation (B18). The final diagrams corresponding the susceptibility $\chi_a^{(5)}$ susceptibility are shown in figures 12, 13. The wavy green lines correspond to the exchange of vacuum photon between oscillators and the wavy red lines correspond the emission and absorption of the same quantum modes on oscillator a. The $\chi^{(5)}$ response can be read off the diagrams. For example, figure 12(I)1, has the form $\langle V_+V_-V_-V_-^{\nu_4}V_-^{\nu_3}V_-^{\nu_2}V_+\rangle$, where $V_-^{\nu_3}V_+^{\nu_2}$ corresponds to the emission and absorption of a photon with oscillator a via the vacuum and cannot be factorized out of the correlation function due to time-ordering. Diagrams that include interactions in-between the emission and absorption of the vacuum photon with the same oscillator vanish when performing the integrations in the susceptibilities (see appendix B).

5. The FWM signal

Assuming monochromatic fields, $E_+^0(\omega)=2\pi\delta(\omega-\omega_i)$, equation (B18) becomes

$$\begin{aligned}
&S^{(3)}(\omega_1,\omega_2,\omega_3)=-2\pi\\
&\quad\times\mathcal{I}\chi^{(3)}(-\omega_3;\omega_1,\omega_2,-\omega_1-\omega_2+\omega_3).
\end{aligned}\tag{25}$$

The simulation of this signal with $\omega_1=\omega_a$ and $\omega_2=\omega_b$ is plotted in figures 8(b)–(m) as a function of ω_3. In figure 8(b), the spectrum shows a single oscillator resonance $\omega_3=\omega_a$. The $\omega_3=\omega_b$ resonance is shown in figure 8(c). The collective resonances at $\omega_3=\omega_b-\omega_a$, $\omega_b+\omega_a$ are shown in figures 8(d), (e), respectively, and have dispersive features.

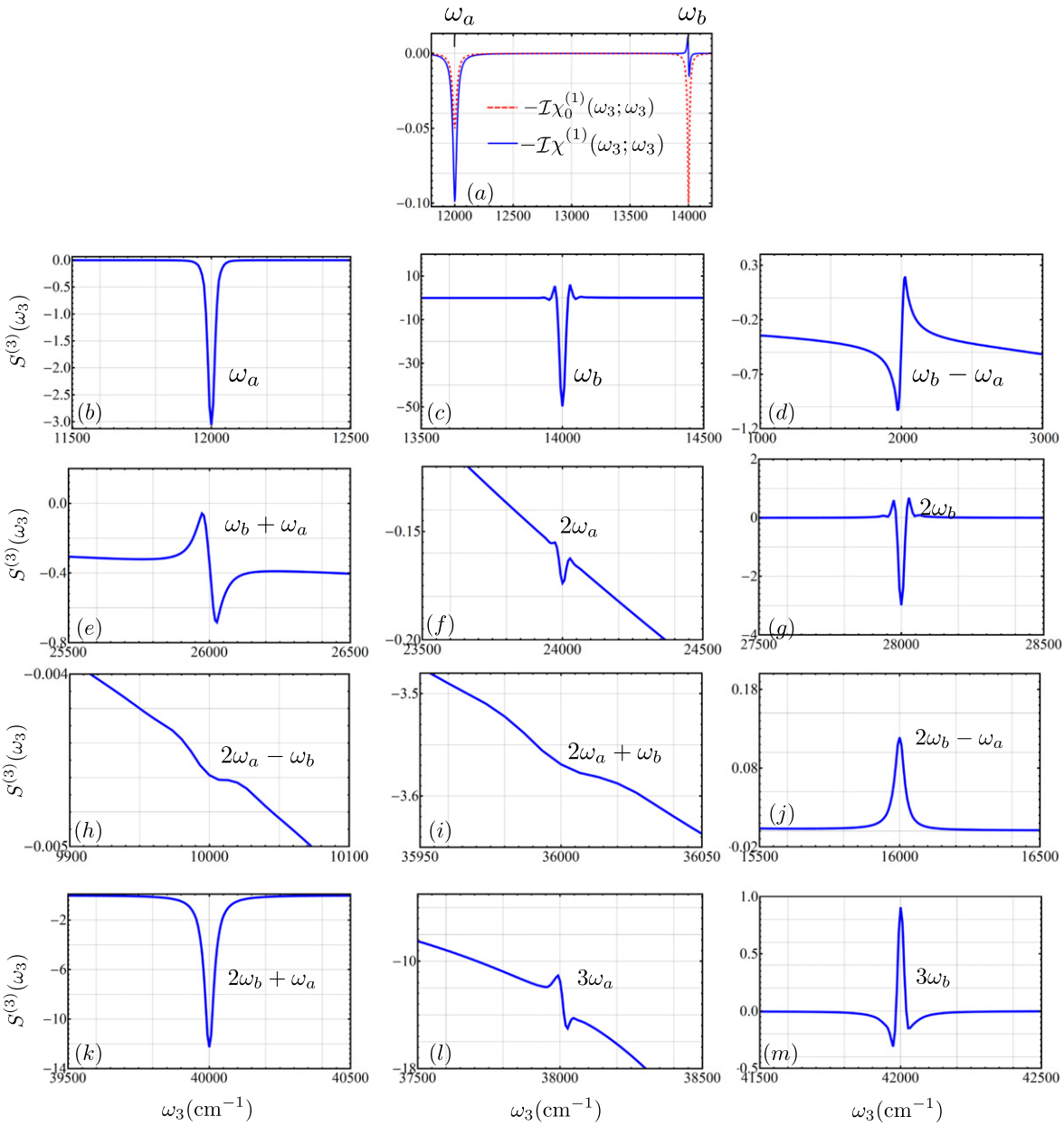

Figure 8. (a) The linear absorption spectrum and the correction to the linear absorption spectrum from coupling to the quantum modes figure 4(a) is shown for comparison. (b)–(m) The FWM spectrum equation (25) $-\mathcal{I}\chi^{(3)}(-\omega_3;\,\omega_1,\,\omega_2,\,-\omega_1-\omega_2+\omega_3)$ is plotted, with $\omega_1=\omega_a$ and $\omega_2=\omega_b$. The spectrum is plotted in arbitrary units and different panels are rescaled.

The double oscillator resonances $\omega_3 = 2\omega_a, 2\omega_b$ are shown in figures 8(f), (g), respectively. The collective peaks at $\omega_3 = 2\omega_a - \omega_b$, $2\omega_a + \omega_b$, are shown in figures 8(h), (i) and have absorption features. Interchanging ω_a and ω_b gives the $\omega_3 = 2\omega_b - \omega_a$, $2\omega_b + \omega_a$ resonances. See figures 8(j), (k), respectively. The triple resonances at $\omega_3 = 3\omega_a$, $3\omega_b$ are shown in figures 8(l), (m), respectively. The resonances $\omega_3 = 2\omega_b + \omega_a$, $2\omega_b - \omega_a$, $2\omega_b$ and $3\omega_b$ occur with the interchange of oscillator a and b in $S(\omega_1, \omega_2, \omega_3)$. For comparison, we include the linear absorption spectrum figure 4(a) in figure 8(a) with the distance between oscillators as $r_{ab}/2\pi\lambda_a = 0.09$. All peak positions in figure 8 can be read off the level scheme in figure 1. The peaks at $\omega_3 = \omega_a, \omega_b$ are the dominant peaks in the FWM spectrum.

In the susceptibility equation (25), we scan the frequency ω_3 that corresponds to the last classical mode at time τ_4 in the diagram of figure 7. A single-particle resonance $\omega_3 = \omega_a$ is measured when the last two interactions are with the classical modes. When there are interactions with quantum modes in-between τ_4 and τ_3 the quantum modes mix the frequency ω_1, ω_2, ω_3 with the matter frequency for oscillator a, creating collective resonances in the spectrum. This can be verified by diagrammatically expanding the susceptibility and using the frequency delta function.

6. The QME misses the optical nonlinearities

We have shown that the coupling to the quantum vacuum field modes affects the response to the classical field $\mathcal{E}_0$. Conventionally, the coupling to the quantum vacuum field modes is described by the QME for the reduced matter density matrix ρ [19, 24].

$$\dot{\rho} = -\frac{\mathrm{i}}{\hbar}\left[H_0 + H_{\mathrm{int}}^0 + H_D, \rho\right] + \sum_{\alpha,\beta}\gamma_{\alpha\beta}\left(B_\beta^\dagger \rho B_\alpha - \frac{1}{2}B_\beta^\dagger B_\alpha \rho - \frac{1}{2}B_\beta^\dagger B_\alpha \rho\right), \tag{26}$$

where $B_\beta^\dagger$ (B_β) are the raising (lowering) operators for the harmonic oscillator

$$H_D = \sum_{\alpha\neq\beta} J_{\alpha\beta} B_\alpha^\dagger B_\beta. \tag{27}$$

$J_{\alpha\beta}$ is the dipole–dipole coupling due to the interaction with the quantum modes and $\gamma_{\alpha\beta}$ is the cooperative spontaneous emission rate, which represents the effective coupling mediated by the exchange of photons [25, 26]. $J_{\alpha\beta}$ and $\gamma_{\alpha\beta}$ are given in equations (14) and (15). The interaction Hamiltonian H_{int}^0 in the rotating wave approximation reads

$$H_{\mathrm{int}}^0 = -\sum_\alpha\left[e\mathcal{E}_0^\dagger(t, \mathbf{r})B_\alpha(t) + e\mathcal{E}_0(t, \mathbf{r})B_\alpha^\dagger(t)\right]. \tag{28}$$

To calculate the optical response using the QME we first compute the expectation value of the displacement and momentum of the βth harmonic oscillator. In second quantization, the dimensionless displacement $\tilde{x} = x\sqrt{\frac{1}{\hbar}\omega m}$ and momentum $\tilde{p} = \frac{p}{\sqrt{\hbar\omega m}}$ of the βth oscillator is given by

$$\tilde{x}_\beta = \frac{1}{\sqrt{2}}\left(B_\beta^\dagger + B_\beta\right), \tag{29}$$

$$\tilde{p}_\beta = -\frac{\mathrm{i}}{\sqrt{2}\hbar}\left(B_\beta^\dagger - B_\beta\right). \tag{30}$$

The expectation value of the operators is

$$\frac{\partial\langle\tilde{x}_\beta\rangle}{\partial t} = \frac{1}{\sqrt{2}}\mathrm{Tr}\left[\left(B_\beta^\dagger + B_\beta\right)\dot{\rho}\right], \tag{31}$$

$$\frac{\partial\langle\tilde{p}_\beta\rangle}{\partial t} = -\frac{\mathrm{i}}{\sqrt{2}\hbar}\mathrm{Tr}\left[\left(B_\beta^\dagger - B_\beta\right)\dot{\rho}\right]. \tag{32}$$

Using the bosonic commutator relations we obtain

$$\frac{\partial\langle\tilde{x}_\beta\rangle}{\partial t} = \omega_\beta\langle\tilde{p}_\beta\rangle + \frac{1}{\hbar}\sum_{\alpha\neq\beta}J_{\alpha\beta}\langle\tilde{p}_\alpha\rangle + \sum_\alpha\gamma_{\alpha\beta}\left(\frac{m_\beta\omega_\beta}{m_\alpha\omega_\alpha}\right)\langle\tilde{x}_\alpha\rangle - \sqrt{2}e\mathcal{I}\mathcal{E}_0(t, r_\beta), \tag{33}$$

$$\frac{\partial\langle\tilde{p}_\beta\rangle}{\partial t} = -\omega_\beta\langle\tilde{x}_\beta\rangle + \frac{1}{\hbar}\sum_{\alpha\neq\beta}J_{\alpha\beta}\langle\tilde{x}_\alpha\rangle + \sum_\alpha\gamma_{\alpha\beta}\langle\tilde{p}_\alpha\rangle - \sqrt{2}\mathrm{i}e\mathcal{R}\mathcal{E}_0(t, r_\beta). \tag{34}$$

We have neglected the Lamb shift by assuming $\omega_\beta^{(0)} \simeq \omega_\beta$. Equations (33) and (34) are linear as expected for a system with a quadratic Hamiltonian. The dipole–dipole interaction $J_{\alpha\beta}$ couples the momentum of one oscillator to displacement coordinates of other. The cooperative rate introduces inter oscillator momentum–momentum and displacement–displacement coupling. The cooperative emission term with $\alpha = \beta$ represents super-radiance contribution.

Equations (33) and (34) can be solved by transformation to the frequency domain. It can be also solved by finding the normal modes (eigenvalues of the system and decoupling the momentum from coordinates). The system of equations is linear with dimensionality $2N$, where N is the number of harmonic oscillators. For e.g., two oscillators one needs to solve four linear equations. This is a generalization of equation (1).

The QME contains sequential photon-exchange, which generates an effective (dipole–dipole) interaction between the oscillators, as well as coupling to vacuum modes, which leads to spontaneous emission. The effective interaction between particles is instantaneous whereas the underlying photon exchange process may be interrupted by other field–matter interactions (this is shown in the latter two diagrams of figure 5 for example). Thus, this calculation shows that the nonlinear response is caused by nonconsecutive photon exchange and is neglected by the QME, since it only includes consecutive processes.

7. Discussion

In summary, we have calculated corrections to the linear and nonlinear response of a harmonic system due to coupling to the vacuum modes of the radiation field. The induced nonlinear response, which is fourth-order in the quantum modes contains two types of processes. The first is the resonant energy transfer between oscillators. It arises when each oscillator a and b interact two times with the quantum modes and this contribution is zero in the heterodyne detected signal for the harmonic system. However, this not true for the homodyne detected signal generated by a coherent spontaneous emission [2] from oscillator a and b. The signal originates from two interactions with the same field mode which is initially in the vaccum state. The diagrammatic expansion is shown in figure 9. In essence, the last two modes acting on oscillator a and b, which are quantum modes, generate the measured signal. The other four quantum modes correspond to the resonant energy transfer process.

In the second process oscillator a interacts three times with the quantum modes and oscillator b interacts once. Here,

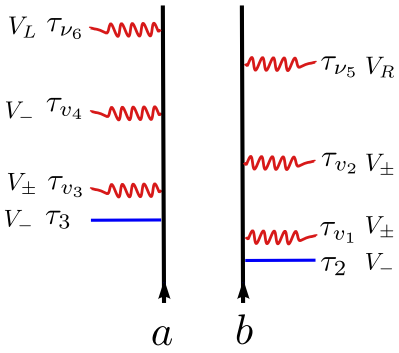

Figure 9. Diagram for the homodyne detected nonlinear response equation (7) expanded to seventh order, six interactions with the quantum modes (wavy red) and two interactions with the classical modes (solid blue) from two uncoupled harmonic oscillators.

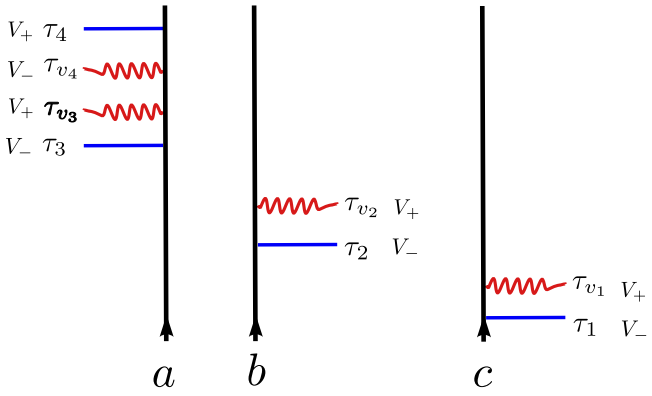

Figure 10. Diagrams for the nonlinear response equation (7) for three uncoupled harmonic oscillators expanded to seventh order, four interactions with the quantum modes (wavy red) and three interactions with the classical modes (solid blue). This contribution to the signal vanishes.

oscillator b emits a photon into the vacuum and oscillator a absorbs it, then oscillator a emits and absorbs the same photon with the vacuum. This process generates the finite nonlinear response. We showed that the FWM spectrum for the heterodyne detected signal contains new collective resonances.

We have calculated the effective $\chi^{(3)}$ generated by the coupling between two harmonic oscillators. It is also possible to envision a three-oscillator process which involves four interactions with the quantum modes and four interactions with the classical modes. This process is shown diagrammatically in figure 10. The last quantum mode on oscillator a at time τ_{v_4} has a V_-. For oscillators b and c, the last quantum mode at times τ_{v_2} and τ_{v_1} be V_+. The interaction at τ_{v_3} can be $V_\pm$. For V_-, $\langle V_+V_-V_-V_-\rangle$ vanishes and for V_+, $\langle E_+E_-E_-E_-\rangle$ vanishes. Thus the nonlinear signal will be composed of two oscillator processes.

Acknowledgments

The support of the National Science Foundation (Grant CHE-1361516), the Chemical Sciences, Geosciences, and Biosciences division, Office of Basic Energy Sciences, Office of Science, US Department of Energy is gratefully acknowledged. RG would like to thank ME Raikh for useful discussions.

Appendix A. Photon-exchange contribution to the linear response

From figure 2, we can immediately write the expression for the photon exchange contribution to the linear absorption spectrum equation (10) as

$$S^{(1)}(\omega) = \mathcal{I}\Bigg[\frac{2\mathrm{i}}{\hbar^4}\int_{-\infty}^{\infty}\mathrm{d}\tau_2\mathrm{e}^{\mathrm{i}\omega\tau_2}\int_{-\infty}^{\tau_2}\mathrm{d}\tau_{v_2} \times\int_{-\infty}^{\tau_{v_2}}\mathrm{d}\tau_{v_1}\int_{-\infty}^{\tau_{v_2}}\mathrm{d}\tau_1\theta(\tau_{v_2}-\tau_{v_1}) \times\Big\{\Big\langle V_L(\tau_2)V_-^{\nu_2}(\tau_{v_2})\Big\rangle_a\Big\langle V_+^{\nu_1}(\tau_{v_1})V_-(\tau_1)\Big\rangle_b$$

$$\times\Big\langle\mathcal{E}_{0\,L}^{\dagger}(\omega,r_b)E_+^{\nu_2}(\tau_{v_2},r_b) \times E_-^{\nu_1}(\tau_{v_1},r_a)E_+^{0}(\tau_1,r_a)\Big\rangle + \Big\langle V_L(\tau_2)V_-^{\nu_2}(\tau_{v_2})V_+^{\nu_1}(\tau_{v_1})V_-(\tau_1)\Big\rangle_a \times\Big\langle\mathcal{E}_{0\,L}^{\dagger}(\omega,r_a)E_+^{\nu_2}(\tau_{v_2},r_a) \times E_-^{\nu_1}(\tau_{v_1},r_a)E_+^{0}(\tau_1,r_a)\Big\rangle\Big\}\Bigg]. \tag{A.1}$$

The classical fields can be pulled out of the correlation function. The signal reads

$$S^{(1)}(\omega) = \mathcal{I}\Bigg[\frac{2\mathrm{i}}{\hbar^4}\sum_{\alpha\beta}\int_{-\infty}^{\infty}\mathrm{d}\tau_2\mathrm{e}^{\mathrm{i}\omega\tau_2}\int_{-\infty}^{\tau_2}\mathrm{d}\tau_{v_2} \times\int_{-\infty}^{\tau_{v_2}}\mathrm{d}\tau_{v_1}\int_{-\infty}^{\tau_{v_2}}\mathrm{d}\tau_1\theta(\tau_{v_2}-\tau_{v_1}) \times\Big\{\Big\langle V_L(\tau_2)V_-^{\nu_2^*}(\tau_{v_2})\Big\rangle_a\Big\langle V_+^{\nu_1}(\tau_{v_1})V_-^{*}(\tau_1)\Big\rangle_b$$

$$\times\mathcal{E}_{0\,L}^{\dagger}(\omega,r_b)E_+^{0}(\tau_1,r_a)\Big\langle E_+^{\nu_2}(\tau_{v_2},r_b)E_-^{\nu_1\,\dagger}(\tau_{v_1},r_a)\Big\rangle + \Big\langle V_L(\tau_2)V_-^{\nu_2^*}(\tau_{v_2})V_+^{\nu_1}(\tau_{v_1})V_-^{*}(\tau_1)\Big\rangle_a \times\mathcal{E}_{0\,L}^{\dagger}\Big(\omega,r_a\Big)E_+^{0}(\tau_1,r_a) \times\Big\langle E_+^{\nu_2}(\tau_{v_2},r_a)E_-^{\nu_1\,\dagger}(\tau_{v_1},r_a)\Big\rangle\Big\}\Bigg]. \tag{A.2}$$

The integrations over time can be done by casting equation (A.2) into the frequency domain and yields

$$S^{(1)}(\omega) = \mathcal{I}\Bigg\{\sum_{\alpha\beta}\frac{2\mathrm{i}}{\hbar^4}\int_{-\infty}^{\infty}\frac{\mathrm{d}\omega_1}{2\pi}\frac{\mathrm{d}\omega_{v_1}}{2\pi}\frac{\mathrm{d}\omega_{v_2}}{2\pi} \times\delta\Big(\omega-\omega_1-\omega_{v_1}+\omega_{v_2}\Big) \times\Big\{\mu_a\mu_b^*\mathcal{E}_0^{\dagger}(\omega,r_a)E_+^{0}(\omega_1,r_b)\vec{\mu}_a^*\vec{\mu}_b$$

$$\times \left\langle E_+^{\nu_2}(\omega_{\nu_2}, r_a), E_-^{\nu_1\,\dagger}(\omega_{\nu_1}, r_b)\right\rangle$$
$$\times G_b(\omega_1)G_a(\omega)G_g(\omega_1-\omega_{\nu_1})$$
$$+ \left|\mu_a\right|^2 \mathcal{E}_0^\dagger(\omega, r_a)E_+^0(\omega_1, r_a)\vec{\mu}_a^*\vec{\mu}_a$$
$$\times \left\langle E_+^{\nu_2}(\omega_{\nu_2}, r_a), E_-^{\nu_1\,\dagger}(\omega_{\nu_1}, r_a)\right\rangle$$
$$\times G_a(\omega_1)G_a(\omega)G_g(\omega_1-\omega_{\nu_1})\Big\}, \tag{A.3}$$

where the Green's function $G_a(\omega)$ is given as $G_a(\omega) = \frac{1}{\omega-\omega_a+\mathrm{i}\Gamma_a}$. Evaluation of the field correlation function can be done by inserting the mode expansion of the fields equation (5), giving

$$\left\langle E_+^{\nu_2}(\tau_{\nu_2}, r_\alpha), E_-^{\nu_1\,\dagger}(\tau_{\nu_1}, r_\beta)\right\rangle = \frac{1}{2}\int\frac{\mathrm{d}\omega}{2\pi}\mathcal{D}_{\alpha\beta}^{(\nu_1,\nu_2)}(\omega) \times\left[\mathrm{e}^{\mathrm{i}\omega(\tau_{\nu_1}-\tau_{\nu_2})} - \mathrm{e}^{-\mathrm{i}\omega(\tau_{\nu_1}-\tau_{\nu_2})}\right],$$
$$\left\langle \mathcal{E}^{\nu_2}\left(\omega_{\nu_2}, \mathbf{r}_\beta\right), \mathcal{E}^{\nu_1\,\dagger}\left(\omega_{\nu_1}, \mathbf{r}_\alpha\right)\right\rangle = \frac{1}{2}\int \mathrm{d}\omega\mathcal{D}_{\alpha\beta}^{(\nu_2,\nu_1)}(\omega) \times\Big[\delta(\omega-\omega_{\nu_1})\delta(\omega-\omega_{\nu_2}) - \delta\left(\omega+\omega_{\nu_1}\right)\delta\left(\omega+\omega_{\nu_2}\right)\Big], \tag{A.4}$$

where

$$\mathcal{D}_{\alpha\beta}^{(i,j)}(\omega) = \frac{\hbar}{2\pi\epsilon_0}\left(-\nabla^2\delta_{ij} + \nabla_i\cdot\nabla_j\right)\frac{\sin(\omega r_{\alpha\beta}/c)}{r_{\alpha\beta}}, \tag{A.5}$$

$r_{\alpha\beta} = |r_\alpha - r_\beta|$ is the distance between oscillators and

$$\mathcal{D}_{\alpha\alpha}^{(l,m)}(\omega) = \frac{\hbar\omega^3}{2\pi\epsilon_0 c^3}\delta_{l,m} \tag{A.6}$$

is the cooperative emission (superradiance). Inserting equations (A.5), (A.6), we can perform two integrations in equation (A.3), using the delta functions.

$$S^{(1)}(\omega) = \mathcal{I}\sum_{\alpha\beta}\Bigg\{\frac{\mathrm{i}\mu_a\mu_b}{2\pi\hbar^2}\mathcal{E}_0^\dagger(\omega, r_b)E_+^0(\omega_1, r_a)G_a(\omega)G_b(\omega) \times\int_{-\infty}^{\infty}\frac{\mathrm{d}\omega_{\nu_1}}{2\pi\hbar^2}\vec{\mu}_a^*\vec{\mu}_b\tilde{\mathcal{D}}_{ab}(\omega_{\nu_1})G_g(\omega-\omega_{\nu_1}) + \frac{\mathrm{i}\left|\mu_a\right|^2}{2\pi\hbar^2}\mathcal{E}_0^\dagger(\omega, r_a)E_+^0(\omega_1, r_a)G_a(\omega)G_a(\omega) \times\int_{-\infty}^{\infty}\frac{\mathrm{d}\omega_{\nu_1}}{2\pi\hbar^2}\vec{\mu}_a^*\vec{\mu}_a\tilde{\mathcal{D}}_{aa}(\omega_{\nu_1})G_g(\omega-\omega_{\nu_1})\Bigg\}. \tag{A.7}$$

The last integration is done using contour integration, which will *select* a particular phase in the sine-function of equation (A.5), $\mathrm{e}^{\mathrm{i}\omega r_{\alpha\beta}/c}$. Using the identity

$$\frac{1}{k^3}\left(-\nabla^2\delta_{ij} + \nabla_i\cdot\nabla_j\right) = \frac{\mathrm{e}^{\mathrm{i}kr}}{r}\left[-\left(\delta_{ij}-\hat{r}_i\hat{r}_j\right)\frac{1}{kr} + \left(\delta_{ij}-3\hat{r}_i\hat{r}_j\right)\left(\frac{-\mathrm{i}}{k^2r^2}+\frac{1}{k^3r^3}\right)\right]\mathrm{e}^{\mathrm{i}kr}. \tag{A.8}$$

Equation (A.9) becomes

$$S^{(1)}(\omega) = \mathcal{I}\sum_{\alpha\beta}\Bigg\{\frac{\mathrm{i}\mu_a\mu_b}{2\pi\hbar^2}\mathcal{E}_0^\dagger(\omega, r_b)E_+^0(\omega_1, r_a)G_a(\omega) \times\frac{J_{\alpha\beta}(r_{\alpha\beta};\omega) - \mathrm{i}\gamma_{\alpha\beta}(r_{\alpha\beta};\omega)}{\hbar\left(\omega-\omega_b+\mathrm{i}\Gamma_b\right)} + \frac{\mathrm{i}\left|\mu_a\right|^2}{2\pi\hbar^2}\mathcal{E}_0^\dagger(\omega, r_a)E_+^0(\omega_1, r_a)G_a(\omega)G_a(\omega) \times\frac{\mu_a^*\mu_a\omega^3}{2\pi\epsilon_0 c^3}\frac{1}{\hbar\left(\omega-\omega_b+\mathrm{i}\Gamma_b\right)}\Bigg\}. \tag{A.9}$$

The effective dipole–dipole coupling $J_{\mathrm{AB}}(r_{\mathrm{AB}};\omega)$ is given as

$$J_{\alpha\beta}(r_{\alpha\beta};\omega) = -\frac{\omega^3}{4\pi\epsilon_0 c^3} \times\left[\left[\left(\vec{\mu}_{g'f}\cdot\vec{\mu}_{\tilde{f}\tilde{g}}\right) - \left(\vec{\mu}_{g'f}\cdot\hat{r}_{\alpha\beta}\right)\left(\vec{\mu}_{\tilde{f}\tilde{g}}\cdot\hat{r}_{\alpha\beta}\right)\right] \times\frac{\cos(\omega r_{\alpha\beta}/c)}{\omega r_{\alpha\beta}/c} - \left[\left(\vec{\mu}_{g'f}\cdot\vec{\mu}_{\tilde{f}\tilde{g}}\right) - 3\left(\vec{\mu}_{g'f}\cdot\hat{r}_{\alpha\beta}\right)\left(\vec{\mu}_{\tilde{f}\tilde{g}}\cdot\hat{r}_{\alpha\beta}\right)\right] \times\left(\frac{\cos(\omega r_{\alpha\beta}/c)}{(\omega r_{\alpha\beta}/c)^3} + \frac{\sin(\omega r_{\alpha\beta}/c)}{(\omega r_{\alpha\beta}/c)^2}\right)\right], \tag{A.10}$$

and the effective corporative emission rate $\gamma_{\alpha\beta}$ is given by

$$\gamma_{\alpha\beta}(r_{\alpha\beta};\omega) = \frac{\omega^3}{4\pi\hbar\epsilon_0 c^3} \times\left[\left[\left(\vec{\mu}_{g'f}\cdot\vec{\mu}_{\tilde{f}\tilde{g}}\right) - \left(\vec{\mu}_{g'f}\cdot\hat{r}_{\alpha\beta}\right)\left(\vec{\mu}_{\tilde{f}\tilde{g}}\cdot\hat{r}_{\alpha\beta}\right)\right] \times\frac{\sin(\omega r_{\alpha\beta}/c)}{\omega r_{\alpha\beta}/c} - \left[\left(\vec{\mu}_{g'f}\cdot\vec{\mu}_{\tilde{f}\tilde{g}}\right) - 3\left(\vec{\mu}_{g'f}\cdot\hat{r}_{\alpha\beta}\right)\left(\vec{\mu}_{\tilde{f}\tilde{g}}\cdot\hat{r}_{\alpha\beta}\right)\right] \times\left(\frac{\sin(\omega r_{\alpha\beta}/c)}{(\omega r_{\alpha\beta}/c)^3} - \frac{\cos(\omega r_{\alpha\beta}/c)}{(\omega r_{\alpha\beta}/c)^2}\right)\right]. \tag{A.11}$$

The vector $\hat{r}$ connects the two dipoles such that their polar angle defines the parallel and perpendicular components as $\mu_{\alpha\parallel} = \mu_\alpha\cos\theta_\alpha$ and $\mu_{\alpha\perp} = \mu_\alpha\sin\theta_\alpha$ and the same for μ_β. See figure 3. Equations (A.10) and (A.11) can be cast in the form of equations (14), (15). From equation (A.9) we can write the effective $\chi^{(1)}$, equation (12).

Appendix B. The nonlinear response to quartic order

In the nonlinear response there are two finite quantum field correlation functions, $\langle E_+E_-E_+E_-\rangle$ and $\langle E_+E_+E_-E_-\rangle$. The field correlation functions $\langle E_+E_-E_-E_\pm\rangle$ vanish.

For bookkeeping purposes, it is convenient to separate the signal according to the possible field correlation functions

$$S^{(3)}(\omega) = \mathcal{S}_I^{(3)}(\omega) + \mathcal{S}_{II}^{(3)}(\omega) + \mathcal{S}_{III}^{(3)}(\omega) + \mathcal{S}_{IV}^{(3)}(\omega). \quad \text{(B.1)}$$

The signal $\mathcal{S}_I^{(3)}(\omega)$ is given diagrammatically in figure 11. The three other signals $\mathcal{S}_{II}^{(3)}(\omega)$-$\mathcal{S}_{IV}^{(3)}(\omega)$ can be deduced from the diagrams in figure 11.

Using the diagrammatic perturbation, we can immediately write the expression corresponding to the diagrams in figure 11

$$\begin{aligned}\mathcal{S}_I^{(3)}(\omega) = &-\mathcal{I}\frac{2}{\hbar}\left(\frac{-\mathrm{i}}{\hbar}\right)^7 \int \mathrm{d}\tau_4 \mathrm{e}^{-\mathrm{i}\omega\tau_4} \int \mathrm{d}\tau_3\mathrm{d}\tau_2\mathrm{d}\tau_1 \\ &\times \int \mathrm{d}\tau_{v_4}\ldots\mathrm{d}\tau_{v_1}\mathcal{E}_L^{0\dagger}(\omega, r_a)E_+^0(\tau_3, r_a)E_+^0(\tau_2, r_a) \\ &\times E_+^0(\tau_1, r_b)\Big\langle E_+^{\nu_4}(\tau_{v_4}, r_a)E_+^{\nu_3}(\tau_{v_3}, r_a) \\ &\times E_-^{\nu_2}(\tau_{v_2}, r_a)E_-^{\nu_1}(\tau_{v_1}, r_b)\Big\rangle \Theta(\tau_{v_2}-\tau_{v_1})\alpha_{+-}^{\nu_1}(\tau_{v_1}, \tau_1) \\ &\times \Big\{\Delta_{+-----+}^{\nu_4\nu_3,\nu_2}(\tau_4, \tau_{v_4}, \tau_3, \tau_{v_3}, \tau_2, \tau_{v_2}) \\ &+ \Delta_{+----+-}^{\nu_4\nu_3,\nu_2}(\tau_4, \tau_3, \tau_2, \tau_{v_4}, \tau_{v_3}, \tau_{v_2}) \\ &+ \Delta_{+--+--}^{\nu_4\nu_3,\nu_2}(\tau_4, \tau_{v_4}, \tau_{v_3}, \tau_{v_2}, \tau_3, \tau_2)\Big\}. \quad \text{(B.2)}\end{aligned}$$

The $\mathcal{S}_{II}^{(3)}(\omega)$ signal has similar diagrams to figure 11, with τ_{v_3} and τ_{v_2} having a V_+, V_-, respectively. The signal is given by

$$\begin{aligned}\mathcal{S}_{II}^{(3)}(\omega) = &-\mathcal{I}\frac{2}{\hbar}\left(\frac{-\mathrm{i}}{\hbar}\right)^7 \int \mathrm{d}\tau_4 \mathrm{e}^{-\mathrm{i}\omega\tau_4} \int \mathrm{d}\tau_3\mathrm{d}\tau_2\mathrm{d}\tau_1 \\ &\times \int \mathrm{d}\tau_{v_4}\ldots\mathrm{d}\tau_{v_1}\mathcal{E}_L^{0\dagger}(\omega, r_a)E_+^0(\tau_3, r_a)E_+^0(\tau_2, r_a) \\ &\times E_+^0(\tau_1, r_b)\Big\langle E_+^{\nu_4}\Big(\tau_{v_4}, r_a\Big)E_-^{\nu_3}\Big(\tau_{v_3}, r_a\Big) \\ &\times E_+^{\nu_2}\Big(\tau_{v_2}, r_a\Big)E_-^{\nu_1}\Big(\tau_{v_1}, r_b\Big)\Big\rangle \Theta(\tau_{v_2}-\tau_{v_1})\alpha_{+-}^{\nu_1}(\tau_{v_1}, \tau_1) \\ &\times \Big\{\Delta_{+--+--}^{\nu_4\nu_3,\nu_2}(\tau_4, \tau_{v_4}, \tau_3, \tau_{v_3}, \tau_2, \tau_{v_2}) \\ &+ \Delta_{+----+-}^{\nu_4\nu_3,\nu_2}(\tau_4, \tau_{v_4}, \tau_3, \tau_2, \tau_{v_3}, \tau_{v_2}) \\ &+ \Delta_{+-+---}^{\nu_4\nu_3,\nu_2}(\tau_4, \tau_{v_4}, \tau_3, \tau_{v_3}, \tau_{v_2}, \tau_2)\Big\}. \quad \text{(B.3)}\end{aligned}$$

The $\mathcal{S}_{III}^{(3)}(\omega)$ signal has similar diagrams to figure 11, with the quantum mode at time τ_{v_1} occurring after τ_{v_2}. The corresponding signal is given as

$$\begin{aligned}\mathcal{S}_{III}^{(3)}(\omega) = &-\mathcal{I}\frac{2}{\hbar}\left(\frac{-\mathrm{i}}{\hbar}\right)^7 \int \mathrm{d}\tau_4 \mathrm{e}^{-\mathrm{i}\omega\tau_4} \int \mathrm{d}\tau_3\mathrm{d}\tau_2\mathrm{d}\tau_1 \\ &\times \int \mathrm{d}\tau_{v_4}\ldots\mathrm{d}\tau_{v_1}\mathcal{E}_L^{0\dagger}(\omega, r_a)E_+^0(\tau_3, r_a)E_+^0(\tau_2, r_a) \\ &\times E_+^0(\tau_1, r_b)\Big\langle E_+^{\nu_4}(\tau_{v_4}, r_a) \\ &\times E_+^{\nu_3}\Big(\tau_{v_3}, r_a\Big)E_-^{\nu_1}(\tau_{v_1}, r_b) \\ &\times E_-^{\nu_2}\Big(\tau_{v_2}, r_a\Big)\Big\rangle \Theta(\tau_{v_3}-\tau_{v_1})\Theta(\tau_{v_1}-\tau_{v_2})\alpha_{+-}^{\nu_1}(\tau_{v_1}, \tau_1) \\ &\times \Big\{\Delta_{+--+--}^{\nu_4\nu_3,\nu_2}(\tau_4, \tau_{v_4}, \tau_3, \tau_{v_3}, \tau_2, \tau_{v_2}) \\ &+ \Delta_{+----+-}^{\nu_4\nu_3,\nu_2}(\tau_4, \tau_3, \tau_2, \tau_{v_4}, \tau_{v_3}, \tau_{v_2})\Big\}. \quad \text{(B.4)}\end{aligned}$$

The $\mathcal{S}_{IV}^{(3)}(\omega)$ signal has similar diagrams to figure 11, with the quantum mode at time τ_{v_1} occurring after time τ_{v_3}. The corresponding signal is given as

$$\begin{aligned}\mathcal{S}_{IV}^{(3)}(\omega) = &-\mathcal{I}\frac{2}{\hbar}\left(\frac{-\mathrm{i}}{\hbar}\right)^7 \int \mathrm{d}\tau_4 \mathrm{e}^{-\mathrm{i}\omega\tau_4} \int \mathrm{d}\tau_3\mathrm{d}\tau_2\mathrm{d}\tau_1 \\ &\times \int \mathrm{d}\tau_{v_4}\ldots\mathrm{d}\tau_{v_1}\mathcal{E}_L^{0\dagger}(\omega, r_a)E_+^0(\tau_3, r_a)E_+^0(\tau_2, r_a) \\ &\times E_+^0(\tau_1, r_b)\Big\langle E_+^{\nu_4}(\tau_{v_4}, r_a)E_-^{\nu_1}(\tau_{v_1}, r_b)E_+^{\nu_3}(\tau_{v_3}, r_a) \\ &\times E_-^{\nu_2}(\tau_{v_2}, r_a)\Big\rangle \Theta(\tau_{v_4}-\tau_{v_1})\Theta(\tau_{v_1}-\tau_{v_3}) \\ &\times \alpha_{+-}^{\nu_1}(\tau_{v_1}, \tau_1)\Big\{\Delta_{+--+--}^{\nu_4\nu_3,\nu_2}(\tau_4, \tau_3, \tau_{v_4}, \tau_{v_3}, \tau_2, \tau_{v_2}) \\ &+ \Delta_{+----+-}^{\nu_4\nu_3,\nu_2}(\tau_4, \tau_3, \tau_{v_4}, \tau_{v_3}, \tau_{v_2}, \tau_2)\Big\}. \quad \text{(B.5)}\end{aligned}$$

The expansion of the field correlation functions is done in appendix C. Inserting the field correlation functions equations (C.11)–(C.14) in equations (B.2)–(B.5), respectively, yields

$$\begin{aligned}\mathcal{S}_I^{(3)}(\omega) = &\mathcal{I}\frac{1}{8\pi^3\hbar^6c^3}\left(\frac{1}{2\pi\epsilon_0}\right)^2 \\ &\times \delta_{\mu\mu'} \int \mathrm{d}\tau_4 \mathrm{e}^{-\mathrm{i}\omega\tau_4} \int \mathrm{d}\tau_3\mathrm{d}\tau_2\mathrm{d}\tau_1 \\ &\times \int \mathrm{d}\tau_{v_4}\ldots\mathrm{d}\tau_{v_1}\mathcal{E}_L^{0\dagger}(\omega, r_a)E_+^0(\tau_3, r_a) \\ &\times E_+^0(\tau_2, r_a)E_+^0(\tau_1, r_b) \\ &\times \Big(-\nabla_{\nu\nu'}^2 + \nabla_\nu\nabla_{\nu'}\Big)\frac{1}{r_{ab}} \\ &\times \Bigg\{\delta^{'''}(\tau_{v_2}-\tau_{v_3})\Bigg[\delta\Bigg(\tau_{v_1}-\tau_{v_4}+\frac{r_{ab}}{c}\Bigg) \\ &- \delta\Bigg(\tau_{v_1}-\tau_{v_4}-\frac{r_{ab}}{c}\Bigg)\Bigg] \\ &+ \delta^{'''}(\tau_{v_2}-\tau_{v_4})\Bigg[\delta\Bigg(\tau_{v_1}-\tau_{v_3}+\frac{r_{ab}}{c}\Bigg) \\ &- \delta\Bigg(\tau_{v_1}-\tau_{v_3}+\frac{r_{ab}}{c}\Bigg]\Bigg\} \\ &\times \Theta\Big(\tau_{v_2}-\tau_{v_1}\Big)\alpha_{+-}^{\nu_1}(\tau_{v_1}, \tau_1) \\ &\times \Big\{\Delta_{+-----+}^{\nu_4\nu_3,\nu_2}(\tau_4, \tau_{v_4}, \tau_3, \tau_{v_3}, \tau_2, \tau_{v_2}) \\ &+ \Delta_{+----+-}^{\nu_4\nu_3,\nu_2}(\tau_4, \tau_3, \tau_2, \tau_{v_4}, \tau_{v_3}, \tau_{v_2}) \\ &+ \Delta_{+--+--}^{\nu_4\nu_3,\nu_2}(\tau_4, \tau_{v_4}, \tau_{v_3}, \tau_{v_2}, \tau_3, \tau_2)\Big\}, \quad \text{(B.6)}\end{aligned}$$

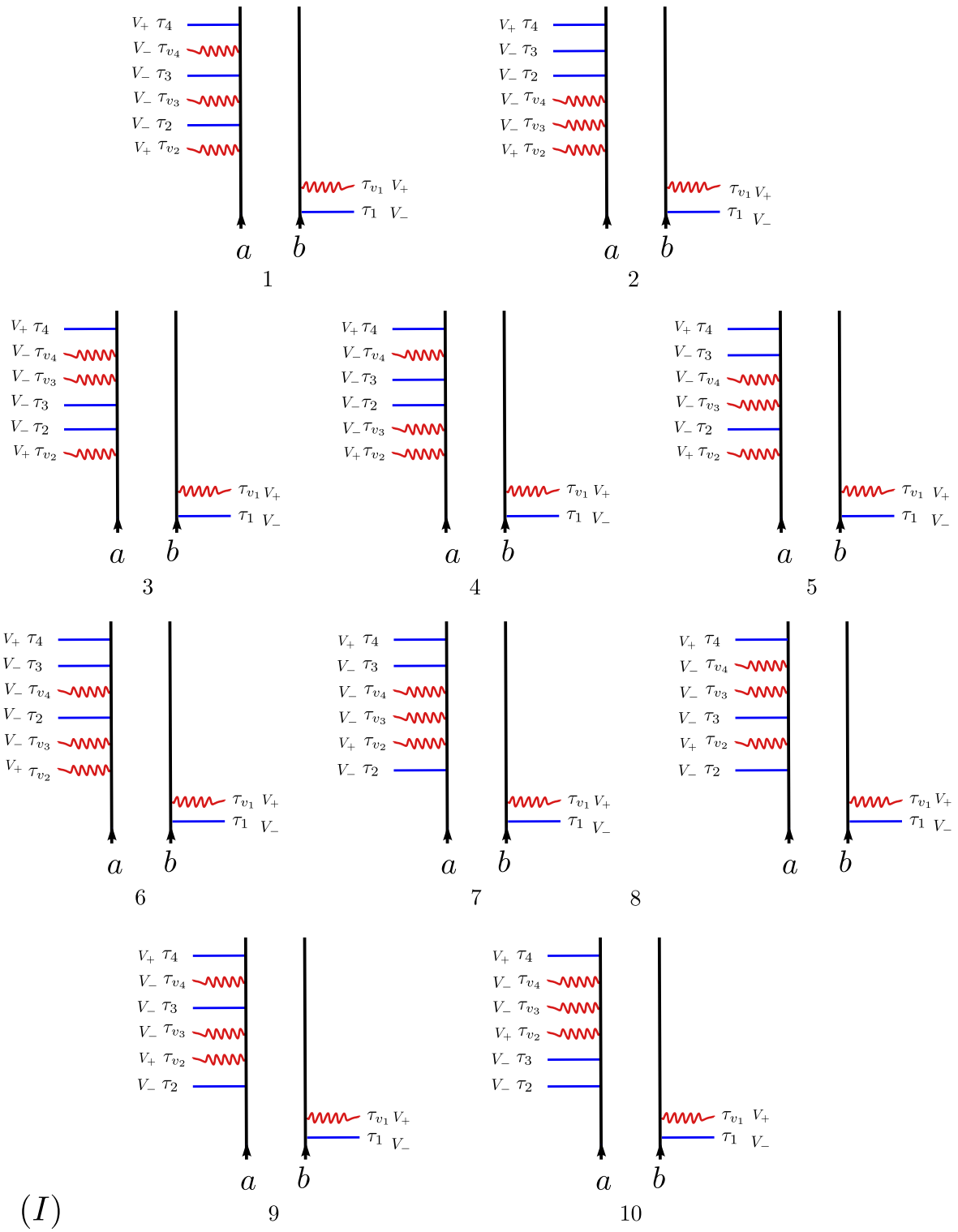

Figure 11. Diagrams for the nonlinear response equation (7) expanded to seventh order, four interactions with the quantum modes (wavy red) and four interactions with the classical modes (solid blue) from two uncoupled harmonic oscillators. The diagrams have the field correlation function $\langle E_+^{\nu_4}(\tau_{v_4}, r_a)E_+^{\nu_3}(\tau_{v_3}, r_a)E_-^{\nu_2}(\tau_{v_2}, r_a)E_-^{\nu_1}(\tau_{v_1}, r_b)\rangle$.

$$
\begin{aligned}
\mathcal{S}_{II}^{(3)}(\omega) = {} & \mathcal{I}\frac{1}{8\pi^3\hbar^6c^3}\left(\frac{1}{2\pi\epsilon_0}\right)^2 \\
& \times \delta_{\mu\mu'}\int \mathrm{d}\tau_4 \mathrm{e}^{-\mathrm{i}\omega\tau_4}\int \mathrm{d}\tau_3\mathrm{d}\tau_2\mathrm{d}\tau_1 \\
& \times \int \mathrm{d}\tau_{\nu_4}\ldots\mathrm{d}\tau_{\nu_1}\mathcal{E}_L^{0\dagger}(\omega, r_a)E_+^0(\tau_3, r_a) \\
& \times E_+^0(\tau_2, r_a)E_+^0(\tau_1, r_b) \\
& \times \left(-\nabla_{\nu\nu'}^2 + \nabla_\nu\nabla_{\nu'}\right)\frac{1}{r_{ab}} \\
& \times \delta^{'''}\left(\tau_{\nu_3} - \tau_{\nu_4}\right)\left[\delta\left(\tau_{\nu_1} - \tau_{\nu_2} + \frac{r_{ab}}{c}\right)\right. \\
& \left. - \delta\left(\tau_{\nu_1} - \tau_{\nu_2} - \frac{r_{ab}}{c}\right)\right] \\
& \times \left\{\Delta_{+--+--}^{\nu_4\nu_3,\nu_2}(\tau_4, \tau_{\nu_4}, \tau_3, \tau_{\nu_3}, \tau_2, \tau_{\nu_2})\right. \\
& + \Delta_{+---+-}^{\nu_4\nu_3,\nu_2}(\tau_4, \tau_{\nu_4}, \tau_3, \tau_2, \tau_{\nu_3}, \tau_{\nu_2}) \\
& \left. + \Delta_{+-+---}^{\nu_4\nu_3,\nu_2}(\tau_4, \tau_{\nu_4}, \tau_3, \tau_{\nu_3}, \tau_{\nu_2}, \tau_2)\right\} \\
& \times \alpha_{+-}^{\nu_1}(\tau_{\nu_1}, \tau_1),
\end{aligned}
\tag{B.7}
$$

$$
\begin{aligned}
\mathcal{S}_{III}^{(3)}(\omega) = {} & \mathcal{I}\frac{1}{8\pi^3\hbar^6c^3}\left(\frac{1}{2\pi\epsilon_0}\right)^2 \\
& \times \delta_{\mu\mu'}\int \mathrm{d}\tau_4 \mathrm{e}^{-\mathrm{i}\omega\tau_4}\int \mathrm{d}\tau_3\mathrm{d}\tau_2\mathrm{d}\tau_1 \\
& \times \int \mathrm{d}\tau_{\nu_4}\ldots\mathrm{d}\tau_{\nu_1}\mathcal{E}_L^{0\dagger}(\omega, r_a)E_+^0(\tau_3, r_a) \\
& \times E_+^0(\tau_2, r_a)E_+^0(\tau_1, r_b) \\
& \times \left(-\nabla_{\nu\nu'}^2 + \nabla_\nu\nabla_{\nu'}\right)\frac{1}{r_{ab}} \\
& \times \left\{\delta^{'''}(\tau_{\nu_2} - \tau_{\nu_4})\left[\delta\left(\tau_{\nu_1} - \tau_{\nu_3} + \frac{r_{ab}}{c}\right)\right.\right. \\
& \left. - \delta\left(\tau_{\nu_1} - \tau_{\nu_3} - \frac{r_{ab}}{c}\right)\right] \\
& + \delta^{'''}(\tau_{\nu_2} - \tau_{\nu_3})\left[\delta\left(\tau_{\nu_1} - \tau_{\nu_4} + \frac{r_{ab}}{c}\right)\right. \\
& \left.\left. - \delta\left(\tau_{\nu_1} - \tau_{\nu_4} - \frac{r_{ab}}{c}\right)\right]\right\}\Theta(\tau_{\nu_3} - \tau_{\nu_1}) \\
& \times \Theta\left(\tau_{\nu_1} - \tau_{\nu_2}\right)\alpha_{+-}^{\nu_1}(\tau_{\nu_1}, \tau_1) \\
& \times \left\{\Delta_{+--+--}^{\nu_4\nu_3,\nu_2}(\tau_4, \tau_{\nu_4}, \tau_3, \tau_{\nu_3}, \tau_2, \tau_{\nu_2})\right. \\
& \left. + \Delta_{+---+-}^{\nu_4\nu_3,\nu_2}(\tau_4, \tau_3, \tau_2, \tau_{\nu_4}, \tau_{\nu_3}, \tau_{\nu_2})\right\},
\end{aligned}
\tag{B.8}
$$

$$
\begin{aligned}
\mathcal{S}_{IV}^{(3)}(\omega) = {} & \mathcal{I}\frac{1}{8\pi^3\hbar^6c^3}\left(\frac{1}{2\pi\epsilon_0}\right)^2 \\
& \times \delta_{\mu\mu'}\int \mathrm{d}\tau_4 \mathrm{e}^{-\mathrm{i}\omega\tau_4}\int \mathrm{d}\tau_3\mathrm{d}\tau_2\mathrm{d}\tau_1 \\
& \times \int \mathrm{d}\tau_{\nu_4}\ldots\mathrm{d}\tau_{\nu_1}\mathcal{E}_L^{0\dagger}(\omega, r_a)E_+^0(\tau_3, r_a) \\
& \times E_+^0(\tau_2, r_a)E_+^0(\tau_1, r_b) \\
& \times \left(-\nabla_{\nu\nu'}^2 + \nabla_\nu\nabla_{\nu'}\right)\frac{1}{r_{ab}} \\
& \times \left[\delta\left(\tau_{\nu_1} - \tau_{\nu_4} + \frac{r_{ab}}{c}\right)\right. \\
& \left. - \delta\left(\tau_{\nu_1} - \tau_{\nu_4} - \frac{r_{ab}}{c}\right)\right] \\
& \times \delta^{'''}(\tau_{\nu_2} - \tau_{\nu_3})\Theta(\tau_{\nu_4} - \tau_{\nu_1}) \\
& \times \Theta(\tau_{\nu_1} - \tau_{\nu_3})\Theta(\tau_{\nu_1} - \tau_{\nu_2}) \\
& \times \alpha_{+-}^{\nu_1}(\tau_{\nu_1}, \tau_1) \\
& \times \left\{\Delta_{+--+--}^{\nu_4\nu_3,\nu_2}(\tau_4, \tau_3, \tau_{\nu_4}, \tau_{\nu_3}, \tau_2, \tau_{\nu_2})\right. \\
& \left. + \Delta_{+---+-}^{\nu_4\nu_3,\nu_2}(\tau_4, \tau_3, \tau_{\nu_4}, \tau_{\nu_3}, \tau_{\nu_2}, \tau_2)\right\}.
\end{aligned}
\tag{B.9}
$$

In equation (B.9) we have inserted the theta function $\Theta(\tau_{\nu_1} - \tau_{\nu_2})$. In the field correlation function of equation (B.9), τ_{ν_1} is always greater than τ_{ν_2} justifying the insertion of this term. The second delta function in equations (B.6)–(B.9) does not contribute since $r_{ab} > 0$, giving

$$
\begin{aligned}
\mathcal{S}_{I}^{(3)}(\omega) = {} & \mathcal{I}\frac{1}{8\pi^3\hbar^6c^3}\left(\frac{1}{2\pi\epsilon_0}\right)^2 \\
& \times \delta_{\mu\mu'}\int \mathrm{d}\tau_4 \mathrm{e}^{-\mathrm{i}\omega\tau_4}\int \mathrm{d}\tau_3\mathrm{d}\tau_2\mathrm{d}\tau_1 \\
& \times \int \mathrm{d}\tau_{\nu_4}\ldots\mathrm{d}\tau_{\nu_1}\mathcal{E}_L^{0\dagger}(\omega, r_a)E_+^0(\tau_3, r_a) \\
& \times E_+^0(\tau_2, r_a)E_+^0(\tau_1, r_b)\left(-\nabla_{\nu\nu'}^2 + \nabla_\nu\nabla_{\nu'}\right)\frac{1}{r_{ab}} \\
& \times \left\{\delta^{'''}(\tau_{\nu_2} - \tau_{\nu_3})\delta\left(\tau_{\nu_1} - \tau_{\nu_4} + \frac{r_{ab}}{c}\right)\right. \\
& \left. + \delta^{'''}(\tau_{\nu_2} - \tau_{\nu_4})\delta\left(\tau_{\nu_1} - \tau_{\nu_3} + \frac{r_{ab}}{c}\right)\right\} \\
& \times \Theta(\tau_{\nu_2} - \tau_{\nu_1})\alpha_{+-}^{\nu_1}(\tau_{\nu_1}, \tau_1) \\
& \times \left\{\Delta_{+----+}^{\nu_4\nu_3,\nu_2}\left(\tau_4, \tau_{\nu_4}, \tau_3, \tau_{\nu_3}, \tau_2, \tau_{\nu_2}\right)\right. \\
& + \Delta_{+---+-}^{\nu_4\nu_3,\nu_2}\left(\tau_4, \tau_3, \tau_2, \tau_{\nu_4}, \tau_{\nu_3}, \tau_{\nu_2}\right) \\
& \left. + \Delta_{+--+--}^{\nu_4\nu_3,\nu_2}(\tau_4, \tau_{\nu_4}, \tau_{\nu_3}, \tau_{\nu_2}, \tau_3, \tau_2)\right\},
\end{aligned}
\tag{B.10}
$$

$$
\begin{aligned}
\mathcal{S}_{II}^{(3)}(\omega) = {} & \mathcal{I}\frac{1}{8\pi^3\hbar^6c^3}\left(\frac{1}{2\pi\epsilon_0}\right)^2 \\
& \times \delta_{\mu\mu'}\int \mathrm{d}\tau_4 \mathrm{e}^{-\mathrm{i}\omega\tau_4}\int \mathrm{d}\tau_3\mathrm{d}\tau_2\mathrm{d}\tau_1 \\
& \times \int \mathrm{d}\tau_{\nu_4}\ldots\mathrm{d}\tau_{\nu_1}\mathcal{E}_L^{0\dagger}(\omega, r_a)E_+^0(\tau_3, r_a) \\
& \times E_+^0(\tau_2, r_a)E_+^0(\tau_1, r_b)\left(-\nabla_{\nu\nu'}^2 + \nabla_\nu\nabla_{\nu'}\right)\frac{1}{r_{ab}} \\
& \times \delta^{'''}(\tau_{\nu_3} - \tau_{\nu_4})\delta\left(\tau_{\nu_1} - \tau_{\nu_2} + \frac{r_{ab}}{c}\right) \\
& \times \left\{\Delta_{+--+--}^{\nu_4\nu_3,\nu_2}(\tau_4, \tau_{\nu_4}, \tau_3, \tau_{\nu_3}, \tau_2, \tau_{\nu_2})\right. \\
& + \Delta_{+---+-}^{\nu_4\nu_3,\nu_2}(\tau_4, \tau_{\nu_4}, \tau_3, \tau_2, \tau_{\nu_3}, \tau_{\nu_2}) \\
& \left. + \Delta_{+-+---}^{\nu_4\nu_3,\nu_2}(\tau_4, \tau_{\nu_4}, \tau_3, \tau_{\nu_3}, \tau_{\nu_2}, \tau_2)\right\} \\
& \times \alpha_{+-}^{\nu_1}(\tau_{\nu_1}, \tau_1),
\end{aligned}
\tag{B.11}
$$

$$\begin{aligned}\mathcal{S}_{III}^{(3)}(\omega) = {} & \mathcal{I}\frac{1}{8\pi^3\hbar^6c^3}\left(\frac{1}{2\pi\epsilon_0}\right)^2 \\ & \times \delta_{\mu\mu'}\int \mathrm{d}\tau_4 \mathrm{e}^{-\mathrm{i}\omega\tau_4}\int \mathrm{d}\tau_3\mathrm{d}\tau_2 d\tau_1 \\ & \times \int \mathrm{d}\tau_{\nu_4}\ldots\mathrm{d}\tau_{\nu_1}\mathcal{E}_L^{0\dagger}(\omega, r_a)E_+^0(\tau_3, r_a) \\ & \times E_+^0(\tau_2, r_a)E_+^0(\tau_1, r_b)\left(-\nabla_{\nu\nu'}^2 + \nabla_\nu\nabla_{\nu'}\right) \\ & \times \frac{1}{r_{ab}}\left\{\delta^{'''}(\tau_{\nu_2}-\tau_{\nu_4})\delta\left(\tau_{\nu_1}-\tau_{\nu_3}+\frac{r_{ab}}{c}\right)\right. \\ & \left. + \delta^{'''}(\tau_{\nu_2}-\tau_{\nu_3})\delta\left(\tau_{\nu_1}-\tau_{\nu_4}+\frac{r_{ab}}{c}\right)\right\} \\ & \times \Theta(\tau_{\nu_3}-\tau_{\nu_1})\Theta(\tau_{\nu_1}-\tau_{\nu_2})\alpha_{+-}^{\nu_1}(\tau_{\nu_1}, \tau_1) \\ & \times \left\{\Delta_{+--+--}^{\nu_4\nu_3,\nu_2}(\tau_4, \tau_{\nu_4}, \tau_3, \tau_{\nu_3}, \tau_2, \tau_{\nu_2})\right. \\ & \left. + \Delta_{+---+-}^{\nu_4\nu_3,\nu_2}(\tau_4, \tau_3, \tau_2, \tau_{\nu_4}, \tau_{\nu_3}, \tau_{\nu_2})\right\}, \end{aligned} \tag{B.12}$$

$$\begin{aligned}\mathcal{S}_{IV}^{(3)}(\omega) = {} & \mathcal{I}\frac{1}{8\pi^3\hbar^6c^3}\left(\frac{1}{2\pi\epsilon_0}\right)^2 \\ & \times \delta_{\mu\mu'}\int \mathrm{d}\tau_4 \mathrm{e}^{-\mathrm{i}\omega\tau_4}\int \mathrm{d}\tau_3\mathrm{d}\tau_2\mathrm{d}\tau_1 \\ & \times \int \mathrm{d}\tau_{\nu_4}\ldots\mathrm{d}\tau_{\nu_1}\mathcal{E}_L^{0\dagger}(\omega, r_a)E_+^0(\tau_3, r_a) \\ & \times E_+^0(\tau_2, r_a)E_+^0(\tau_1, r_b)\left(-\nabla_{\nu\nu'}^2 + \nabla_\nu\nabla_{\nu'}\right)\frac{1}{r_{ab}} \\ & \times \delta\left(\tau_{\nu_1}-\tau_{\nu_4}+\frac{r_{ab}}{c}\right)\delta^{'''}(\tau_{\nu_2}-\tau_{\nu_3})\Theta(\tau_{\nu_4}-\tau_{\nu_1}) \\ & \times \Theta(\tau_{\nu_1}-\tau_{\nu_3})\Theta(\tau_{\nu_1}-\tau_{\nu_2})\alpha_{+-}^{\nu_1}(\tau_{\nu_1}, \tau_1) \\ & \times \left\{\Delta_{+--+--}^{\nu_4\nu_3,\nu_2}(\tau_4, \tau_3, \tau_{\nu_4}, \tau_{\nu_3}, \tau_2, \tau_{\nu_2})\right. \\ & \left. + \Delta_{+---+-}^{\nu_4\nu_3,\nu_2}(\tau_4, \tau_3, \tau_{\nu_4}, \tau_{\nu_3}, \tau_{\nu_2}, \tau_2)\right\}. \end{aligned} \tag{B.13}$$

Equations (B.12) and (B.13) can be added yielding

$$\begin{aligned}\mathcal{S}_{III}^{(3)}(\omega) + \mathcal{S}_{IV}^{(3)}(\omega) & \\ = {} & \mathcal{I}\frac{1}{8\pi^3\hbar^6c^3}\left(\frac{1}{2\pi\epsilon_0}\right)^2 \\ & \times \delta_{\mu\mu'}\int \mathrm{d}\tau_4 \mathrm{e}^{-\mathrm{i}\omega\tau_4}\int \mathrm{d}\tau_3\mathrm{d}\tau_2\mathrm{d}\tau_1 \\ & \times \int \mathrm{d}\tau_{\nu_4}\ldots\mathrm{d}\tau_{\nu_1}\mathcal{E}_L^{0\dagger}(\omega, r_a) \\ & \times E_+^0(\tau_3, r_a)E_+^0(\tau_2, r_a) \\ & \times E_+^0(\tau_1, r_b)\Theta(\tau_{\nu_1}-\tau_{\nu_2})\left(-\nabla_{\nu\nu'}^2 + \nabla_\nu\nabla_{\nu'}\right)\frac{1}{r_{ab}} \\ & \times \left\{\delta^{'''}(\tau_{\nu_2}-\tau_{\nu_4})\delta\left(\tau_{\nu_1}-\tau_{\nu_3}+\frac{r_{ab}}{c}\right)\right. \\ & \left. + \delta\left(\tau_{\nu_1}-\tau_{\nu_4}+\frac{r_{ab}}{c}\right)\delta^{'''}(\tau_{\nu_2}-\tau_{\nu_3})\right\} \\ & \times \left\{\Delta_{+--+--}^{\nu_4\nu_3,\nu_2}(\tau_4, \tau_{\nu_4}, \tau_3, \tau_{\nu_3}, \tau_2, \tau_{\nu_2})\right. \\ & \left. + \Delta_{+---+-}^{\nu_4\nu_3,\nu_2}(\tau_4, \tau_3, \tau_2, \tau_{\nu_4}, \tau_{\nu_3}, \tau_{\nu_2})\right\} \\ & \times \alpha_{+-}^{\nu_1}(\tau_{\nu_1}, \tau_1). \end{aligned} \tag{B.14}$$

The term $\Delta_{+----+}^{\nu_4\nu_3,\nu_2}$ is absent for equation (B.14). This is because $\Delta_{+----+}^{\nu_4\nu_3,\nu_2}$ corresponds to an interaction with quantum fields before the classical fields. This term vanishes, since we assume that the quantum fields are initially in the ground state. We can freely insert $\Delta_{+----+}^{\nu_4\nu_3,\nu_2}$, since it is zero, into equation (B.14) and add $\mathcal{S}_I(\omega)$, $\mathcal{S}_{III}(\omega)$ and $\mathcal{S}_{IV}(\omega)$, yielding

$$\begin{aligned}\mathcal{S}_I^{(3)}(\omega) + \mathcal{S}_{III}^{(3)}(\omega) + \mathcal{S}_{IV}^{(3)}(\omega) & \\ = {} & \mathcal{I}\frac{1}{8\pi^3\hbar^6c^3}\left(\frac{1}{2\pi\epsilon_0}\right)^2 \\ & \times \delta_{\mu\mu'}\int \mathrm{d}\tau_4 \mathrm{e}^{-\mathrm{i}\omega\tau_4}\int \mathrm{d}\tau_3\mathrm{d}\tau_2\mathrm{d}\tau_1\int \mathrm{d}\tau_{\nu_4}\ldots\mathrm{d}\tau_{\nu_1} \\ & \times \mathcal{E}_L^{0\dagger}(\omega, r_a)E_+^0(\tau_3, r_a)E_+^0(\tau_2, r_a) \\ & \times E_+^0(\tau_1, r_b)\left(-\nabla_{\nu\nu'}^2 + \nabla_\nu\nabla_{\nu'}\right)\frac{1}{r_{ab}} \\ & \times \left\{\delta^{'''}(\tau_{\nu_2}-\tau_{\nu_3})\delta\left(\tau_{\nu_1}-\tau_{\nu_4}+\frac{r_{ab}}{c}\right)\right. \\ & \left. + \delta\left(\tau_{\nu_1}-\tau_{\nu_3}+\frac{r_{ab}}{c}\right)\delta^{'''}(\tau_{\nu_2}-\tau_{\nu_4})\right\} \\ & \times \left\{\Delta_{+----+}^{\nu_4\nu_3,\nu_2}(\tau_4, \tau_{\nu_4}, \tau_3, \tau_{\nu_3}, \tau_2, \tau_{\nu_2})\right. \\ & + \Delta_{+---+-}^{\nu_4\nu_3,\nu_2}(\tau_4, \tau_3, \tau_2, \tau_{\nu_4}, \tau_{\nu_3}, \tau_{\nu_2}) \\ & \left. + \Delta_{+--+--}^{\nu_4\nu_3,\nu_2}(\tau_4, \tau_{\nu_4}, \tau_{\nu_3}, \tau_{\nu_2}, \tau_3, \tau_2)\right\} \\ & \times \alpha_{+-}^{\nu_1}(\tau_{\nu_1}, \tau_1). \end{aligned} \tag{B.15}$$

The total signal can be found by adding equations (B.11) and (B.15), yielding

$$\begin{aligned}S^{(3)}(\omega) = {} & \mathcal{I}\frac{1}{8\pi^3\hbar^6c^3}\left(\frac{1}{2\pi\epsilon_0}\right)^2\int \mathrm{d}\tau_4 \mathrm{e}^{-\mathrm{i}\omega\tau_4} \\ & \times \int \mathrm{d}\tau_3\mathrm{d}\tau_2\mathrm{d}\tau_1\int \mathrm{d}\tau_{\nu_4}\ldots\mathrm{d}\tau_{\nu_1}\mathcal{E}_L^{0\dagger}(\omega, r_a)E_+^0(\tau_3, r_a) \\ & \times E_+^0(\tau_2, r_a)E_+^0(\tau_1, r_b)\left(-\nabla_{\nu\nu'}^2 + \nabla_\nu\nabla_{\nu'}\right) \\ & \times \frac{1}{r_{ab}}\delta_{\mu\mu'}\left\{\left[\delta^{'''}(\tau_{\nu_2}-\tau_{\nu_3})\delta\left(\tau_{\nu_1}-\tau_{\nu_4}+\frac{r_{ab}}{c}\right)\right.\right. \\ & \left. + \delta^{'''}(\tau_{\nu_2}-\tau_{\nu_4})\delta\left(\tau_{\nu_1}-\tau_{\nu_3}+\frac{r_{ab}}{c}\right)\right. \\ & \times \left[\Delta_{+----+}^{\nu_4\nu_3,\nu_2}(\tau_4, \tau_{\nu_4}, \tau_3, \tau_{\nu_3}, \tau_2, \tau_{\nu_2})\right. \\ & + \Delta_{+---+-}^{\nu_4\nu_3,\nu_2}(\tau_4, \tau_3, \tau_2, \tau_{\nu_4}, \tau_{\nu_3}, \tau_{\nu_2}) \\ & \left. + \Delta_{+--+--}^{\nu_4\nu_3,\nu_2}(\tau_4, \tau_{\nu_4}, \tau_{\nu_3}, \tau_{\nu_2}, \tau_3, \tau_2)\right] \\ & \times \delta^{'''}(\tau_{\nu_3}-\tau_{\nu_4}) + \delta\left(\tau_{\nu_1}-\tau_{\nu_2}+\frac{r_{ab}}{c}\right) \\ & \times \left\{\Delta_{+--+--}^{\nu_4\nu_3,\nu_2}(\tau_4, \tau_{\nu_4}, \tau_3, \tau_{\nu_3}, \tau_2, \tau_{\nu_2})\right. \\ & + \Delta_{+---+-}^{\nu_4\nu_3,\nu_2}(\tau_4, \tau_{\nu_4}, \tau_3, \tau_2, \tau_{\nu_3}, \tau_{\nu_2}) \\ & \left. + \Delta_{+-+---}^{\nu_4\nu_3,\nu_2}(\tau_4, \tau_{\nu_4}, \tau_3, \tau_{\nu_3}, \tau_{\nu_2}, \tau_2)\right\} \\ & \times \alpha_{+-}^{\nu_1}(\tau_{\nu_1}, \tau_1). \end{aligned} \tag{B.16}$$

Using equations (C.9) and (C.10), equation (B.16) can be cast into the following form

$$
\begin{aligned}
S^{(3)}(\omega) = &-\frac{2}{\hbar}\left(\frac{-\mathrm{i}}{\hbar}\right)^7 \int \mathrm{d}\tau_4 \mathrm{e}^{-\mathrm{i}\omega\tau_4} \\
&\times \int \mathrm{d}\tau_3 \mathrm{d}\tau_2 \mathrm{d}\tau_1 \int \mathrm{d}\tau_{\nu_4} \ldots \mathrm{d}\tau_{\nu_1} \mathcal{E}_L^{0\dagger} \\
&\times (\omega, r_a) E_+^0(\tau_3, r_a) E_+^0(\tau_2, r_a) \\
&\times E_+^0(\tau_1, r_b) \frac{\hbar}{\mu_a \mu_b} \int \frac{\mathrm{d}\omega_{\nu_1}}{2\pi} \\
&\times \left[J_{ab}\left(r_{ab}; \omega_{\nu_1}\right) - \mathrm{i}\gamma_{ab}\left(r_{ab}; \omega_{\nu_1}\right) \right] \\
&\times \int \frac{\mathrm{d}\omega_{\nu_2}}{2\pi} \tilde{D}_{aa}^{(\mu,\mu')}(\omega_{\nu_2}) \\
&\times \Big\{ \Big[\mathrm{e}^{\mathrm{i}\omega_{\nu_2}(\tau_{\nu_2}-\tau_{\nu_3}) + \mathrm{i}\omega_{\nu_1}(\tau_{\nu_1}-\tau_{\nu_4})} \\
&+ \mathrm{e}^{\mathrm{i}\omega_{\nu_2}(\tau_{\nu_2}-\tau_{\nu_4}) + \mathrm{i}\omega_{\nu_1}(\tau_{\nu_1}-\tau_{\nu_3})} \Big] \\
&\times \Big[\Delta_{+-----+}^{\nu_4\nu_3,\nu_2}(\tau_4, \tau_{\nu_4}, \tau_3, \tau_{\nu_3}, \tau_2, \tau_{\nu_2}) \\
&+ \Delta_{+----+-}^{\nu_4\nu_3,\nu_2}(\tau_4, \tau_3, \tau_2, \tau_{\nu_4}, \tau_{\nu_3}, \tau_{\nu_2}) \\
&+ \Delta_{+---+--}^{\nu_4\nu_3,\nu_2}(\tau_4, \tau_{\nu_4}, \tau_{\nu_3}, \tau_{\nu_2}, \tau_3, \tau_2) \Big] \\
&+ \mathrm{e}^{\mathrm{i}\omega_{\nu_2}(\tau_{\nu_3}-\tau_{\nu_4}) + \mathrm{i}\omega_{\nu_1}(\tau_{\nu_1}-\tau_{\nu_2})} \\
&\times \Big[\Delta_{+--+--}^{\nu_4\nu_3,\nu_2}(\tau_4, \tau_{\nu_4}, \tau_3, \tau_{\nu_3}, \tau_2, \tau_{\nu_2}) \\
&+ \Delta_{+----+-}^{\nu_4\nu_3,\nu_2}(\tau_4, \tau_{\nu_4}, \tau_3, \tau_2, \tau_{\nu_3}, \tau_{\nu_2}) \\
&+ \Delta_{+-+---}^{\nu_4\nu_3,\nu_2}(\tau_4, \tau_{\nu_4}, \tau_3, \tau_{\nu_3}, \tau_{\nu_2}, \tau_2) \Big] \Big\} \\
&\times \alpha_{+-}^{\nu_1}(\tau_{\nu_1}, \tau_1),
\end{aligned}
\tag{B.17}
$$

where $J_{ab}(r_{ab}; \omega_{\nu_1})$ and $\gamma_{ab}(r_{ab}; \omega_{\nu_1})$ are given by equations (14) and (15), respectively. Next we use the Fourier transform $\mathcal{E}(t) = \int_{-\infty}^{\infty} \frac{\mathrm{d}\omega}{2\pi} \mathcal{E}(\omega) \mathrm{e}^{-\mathrm{i}\omega t}$ to perform the integrations over time, which yields

$$
\begin{aligned}
S^{(3)}(\omega) = &-\mathcal{I}\mathcal{E}_L^{0\dagger}(\omega, r_a) \\
&\times \int \frac{\mathrm{d}\omega_3}{2\pi} \frac{\mathrm{d}\omega_2}{2\pi} \frac{\mathrm{d}\omega_1}{2\pi} E_+^0(\omega_3, r_a) \\
&\times E_+^0(\omega_2, r_a) E_+^0(\omega_1, r_b) \\
&\times \chi^{(3)}(-\omega; \omega_1, \omega_2, \omega_3)
\end{aligned}
\tag{B.18}
$$

with the susceptibility given as

$$
\begin{aligned}
&\chi^{(3)}(-\omega; \omega_1, \omega_2, \omega_3) \\
&= \left(\frac{1}{2\pi\hbar}\right)^8 \frac{\hbar}{\mu_a \mu_b} \int \mathrm{d}\omega_{\nu_1} \mathrm{d}\omega_{\nu_2} \tilde{D}_{aa}^{(\mu,\mu')}(\omega_{\nu_1}) \\
&\quad \times \left[J_{ab}\left(r_{ab}; \omega_{\nu_2}\right) - \mathrm{i}\gamma_{ab}\left(r_{ab}; \omega_{\nu_2}\right) \right] \\
&\quad \times \Big\{ \chi_{+-----+}^{\nu_1\nu_2,\nu_2}(\omega, \omega_{\nu_1}, \omega_3, \omega_{\nu_2}, \omega_2, \omega_{\nu_2}) \\
&\quad + \chi_{+----+-}^{\nu_1\nu_2,\nu_2}(\omega, \omega_3, \omega_2, \omega_{\nu_1}, \omega_{\nu_2}, \omega_{\nu_2}) \\
&\quad + \chi_{+---+--}^{\nu_1\nu_2,\nu_2}(\omega, \omega_{\nu_1}, \omega_{\nu_2}, \omega_{\nu_2}, \omega_3, \omega_2) \\
&\quad + \chi_{+-----+}^{\nu_2\nu_1,\nu_2}(\omega, \omega_{\nu_2}, \omega_3, \omega_{\nu_1}, \omega_2, \omega_{\nu_2}) \\
&\quad + \chi_{+----+-}^{\nu_2\nu_1,\nu_2}(\omega, \omega_3, \omega_2, \omega_{\nu_2}, \omega_{\nu_1}, \omega_{\nu_2}) \\
&\quad + \chi_{+---+--}^{\nu_2\nu_1,\nu_2}(\omega, \omega_{\nu_2}, \omega_{\nu_1}, \omega_{\nu_2}, \omega_3, \omega_2) \\
&\quad + \chi_{+---+--}^{\nu_2\nu_2,\nu_1}(\omega, \omega_{\nu_2}, \omega_{\nu_2}, \omega_{\nu_1}, \omega_3, \omega_2) \\
&\quad + \chi_{+----+-}^{\nu_2\nu_2,\nu_1}(\omega, \omega_3, \omega_2, \omega_{\nu_2}, \omega_{\nu_2}, \omega_{\nu_1}) \\
&\quad + \chi_{+-+---}^{\nu_2\nu_2,\nu_1}(\omega, \omega_{\nu_2}, \omega_3, \omega_{\nu_2}, \omega_{\nu_1}, \omega_2) \Big\},
\end{aligned}
\tag{B.19}
$$

where the susceptibilities $\chi_{+-----+}^{\nu_i\nu_j,\nu_k}$, $\chi_{+----+-}^{\nu_i\nu_j,\nu_k}$, $\chi_{+---+--}^{\nu_i\nu_j,\nu_k}$, $\chi_{+-+---}^{\nu_i\nu_j,\nu_k}$ are given in equations (19)–(22), respectively.

The integrations over ω_{ν_1} and ω_{ν_2} are done using contour integration. The contour integration over ω_{ν_2} vanishes for the diagrams in figure 11 that have quantum and classical field interactions in-between the emission and absorption of the same photon with oscillator a. With this observation, we can eliminate the diagrams that contain interactions with the field in-between the emission and absorption of a photon by oscillator a via the vacuum. This is done in figures 12–13, where we draw all diagrams which contribute to the signal. The green wavy lines correspond to the emission of a quantum mode from oscillator b and the absorption by oscillator a. The red wavy lines correspond to the emission and absorption of a photon by oscillator a via the vacuum.

In diagrams figures 12(1), (4), (6) it is possible to have τ_{ν_4} and τ_{ν_3} red and τ_{ν_2} and τ_{ν_1} green. However, this contribution vanishes in the expansion of the field correlation function, because it corresponds to $\langle E_+ E_- E_- E_+ \rangle$, which vanishes.

The final expression of the susceptibility for diagrams in figures 12–13 is given as equation (18).

Appendix C. The field correlation function

The field correlation functions can be expanded using the expression for the field equation (5) and Wick's theorem giving

$$
\begin{aligned}
&\left\langle E_+^{\nu_4}(\tau_{\nu_4}, r_a) E_+^{\nu_3}(\tau_{\nu_3}, r_a) E_-^{\nu_2}(\tau_{\nu_2}, r_a) E_-^{\nu_1}(\tau_{\nu_1}, r_b) \right\rangle \\
&= \int \frac{\mathrm{d}\omega_{\nu_1}}{2\pi} D_{ab}^{(\nu,\nu')}(\omega_{\nu_1}) \int \frac{\mathrm{d}\omega_{\nu_2}}{2\pi} D_{aa}^{(\mu,\mu')}(\omega_{\nu_2}) \\
&\quad \times \Big\{ \Big[\mathrm{e}^{\mathrm{i}\omega_{\nu_2}(\tau_{\nu_2}-\tau_{\nu_3})} - \mathrm{e}^{\mathrm{i}\omega_{\nu_2}(\tau_{\nu_3}-\tau_{\nu_2})} \Big] \\
&\quad \times \Big[\mathrm{e}^{\mathrm{i}\omega_{\nu_1}(\tau_{\nu_1}-\tau_{\nu_4})} - \mathrm{e}^{\mathrm{i}\omega_{\nu_1}(\tau_{\nu_4}-\tau_{\nu_1})} \Big] \\
&\quad + \Big[\mathrm{e}^{\mathrm{i}\omega_{\nu_2}(\tau_{\nu_2}-\tau_{\nu_4})} - \mathrm{e}^{\mathrm{i}\omega_{\nu_2}(\tau_{\nu_4}-\tau_{\nu_2})} \Big] \\
&\quad \times \Big[\mathrm{e}^{\mathrm{i}\omega_{\nu_1}(\tau_{\nu_1}-\tau_{\nu_3})} - \mathrm{e}^{\mathrm{i}\omega_{\nu_1}(\tau_{\nu_3}-\tau_{\nu_1})} \Big] \Big\},
\end{aligned}
\tag{C.1}
$$

$$
\begin{aligned}
&\left\langle E_+^{\nu_4}(\tau_{\nu_4}, r_a) E_-^{\nu_3}(\tau_{\nu_3}, r_a) E_+^{\nu_2}(\tau_{\nu_2}, r_a) E_-^{\nu_1}(\tau_{\nu_1}, r_b) \right\rangle \\
&= \int \frac{\mathrm{d}\omega_{\nu_1}}{2\pi} D_{ab}^{(\nu,\nu')}(\omega_{\nu_1}) \int \frac{\mathrm{d}\omega_{\nu_2}}{2\pi} D_{aa}^{(\mu,\mu')}(\omega_{\nu_3}) \\
&\quad \times \Big\{ \Big[\mathrm{e}^{\mathrm{i}\omega_{\nu_3}(\tau_{\nu_3}-\tau_{\nu_4})} - \mathrm{e}^{\mathrm{i}\omega_{\nu_3}(\tau_{\nu_4}-\tau_{\nu_3})} \Big] \\
&\quad \times \Big[\mathrm{e}^{\mathrm{i}\omega_{\nu_1}(\tau_{\nu_1}-\tau_{\nu_2})} - \mathrm{e}^{\mathrm{i}\omega_{\nu_1}(\tau_{\nu_2}-\tau_{\nu_1})} \Big] \Big\},
\end{aligned}
\tag{C.2}
$$

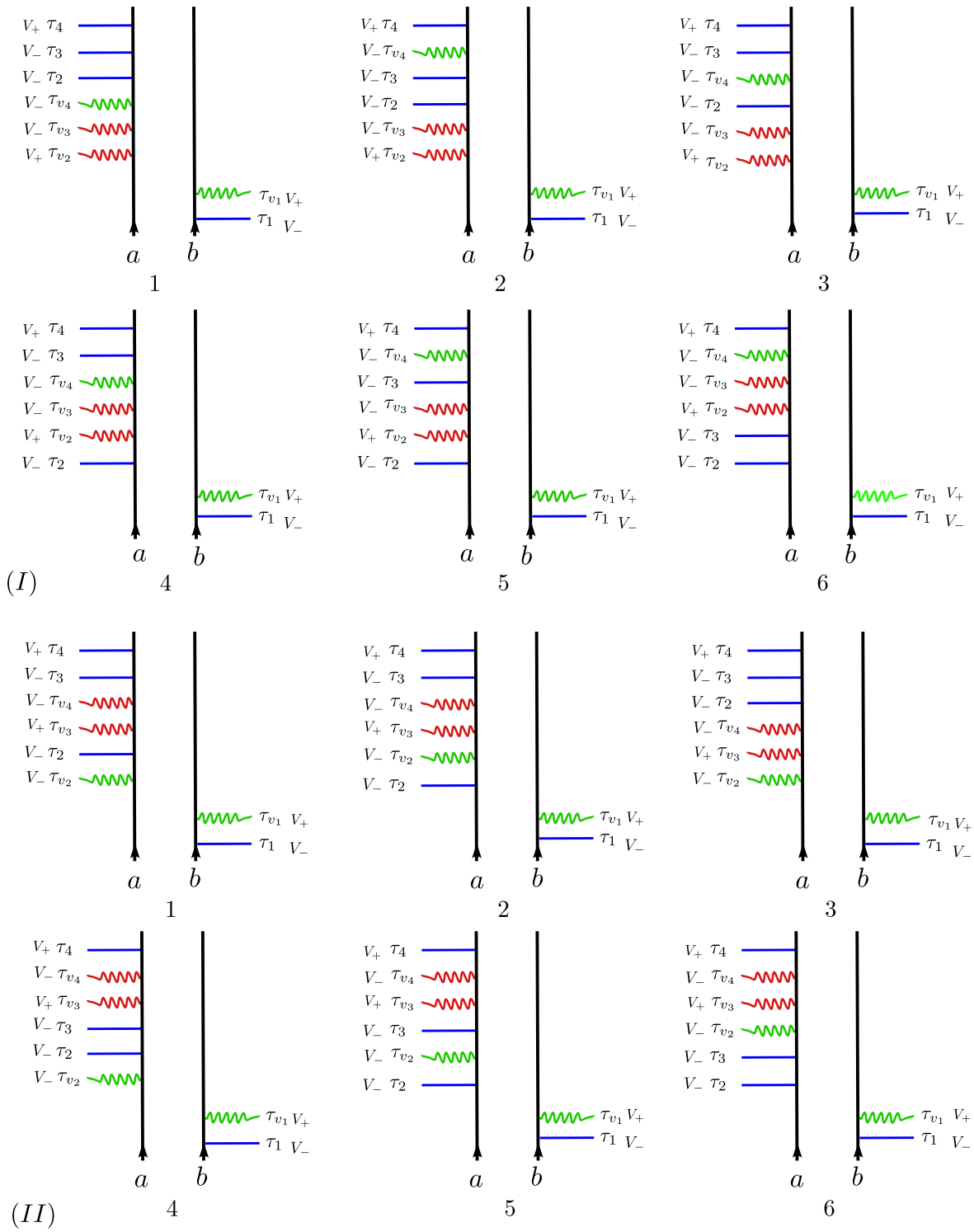

Figure 12. Similar to figure 11, the diagrams that vanish after the contour integration ω_{ν_2} in equation (B19) have been dropped. The red wavy lines correspond to the emission and absorption of a photon with oscillator a. The green wavy lines to the emission of a photon from oscillator b and the absorption the photon by oscillator a. The diagrams proportional to (I) $\langle E_+^{\nu_4}(\tau_{\nu_4}, r_a)E_+^{\nu_3}(\tau_{\nu_3}, r_a)E_-^{\nu_2}(\tau_{\nu_2}, r_a)E_-^{\nu_1}(\tau_{\nu_1}, r_b)\rangle$. (II) $\langle E_+^{\nu_4}(\tau_{\nu_4}, r_a)E_+^{\nu_3}(\tau_{\nu_3}, r_a)E_-^{\nu_1}(\tau_{\nu_1}, r_b)E_-^{\nu_2}(\tau_{\nu_2}, r_a)\rangle$.

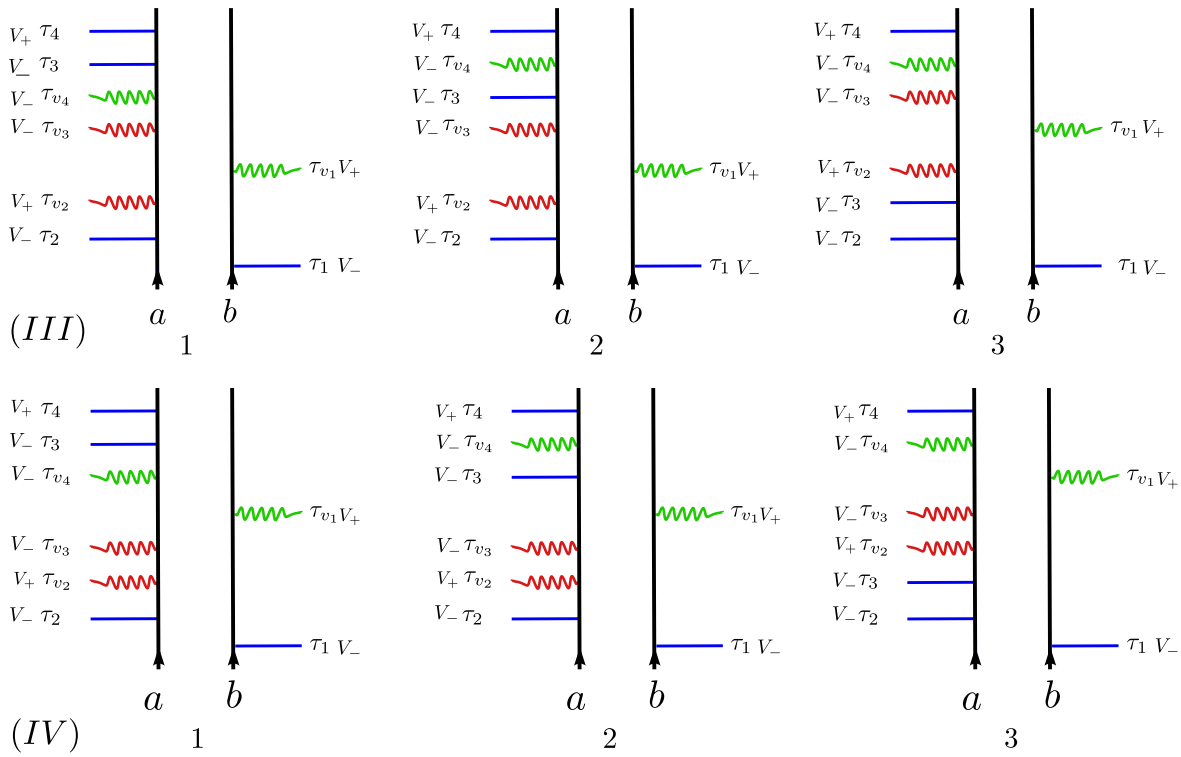

Figure 13. Similar to figure 12 with the field correlation function (III) $\langle E_+^{\nu_4}(\tau_{v_4}, r_a)E_+^{\nu_3}(\tau_{v_3}, r_a)E_-^{\nu_1}(\tau_{v_1}, r_b)E_-^{\nu_2}(\tau_{v_2}, r_a)\rangle$ (IV) $\langle E_+^{\nu_4}(\tau_{v_4}, r_a)E_-^{\nu_1}(\tau_{v_1}, r_b)E_+^{\nu_3}(\tau_{v_3}, r_a)E_-^{\nu_2}(\tau_{v_2}, r_a)\rangle$.

$$\begin{aligned}\left\langle E_+^{\nu_4}(\tau_{v_4}, r_a)E_+^{\nu_3}(\tau_{v_3}, r_a)E_-^{\nu_1}(\tau_{v_1}, r_b)E_-^{\nu_2}(\tau_{v_2}, r_a)\right\rangle &= \int\frac{\mathrm{d}\omega_{v_2}}{2\pi}\mathcal{D}_{aa}^{(\nu,\nu')}(\omega_{v_2})\int\frac{\mathrm{d}\omega_{v_1}}{2\pi}\mathcal{D}_{ab}^{(\mu,\mu')}(\omega_{v_1})\\ &\times\left\{\left[\mathrm{e}^{\mathrm{i}\omega_{v_1}(\tau_{v_1}-\tau_{v_3})}-\mathrm{e}^{\mathrm{i}\omega_{v_1}(\tau_{v_3}-\tau_{v_1})}\right]\right.\\ &\times\left[\mathrm{e}^{\mathrm{i}\omega_{v_2}(\tau_{v_2}-\tau_{v_4})}-\mathrm{e}^{\mathrm{i}\omega_{v_2}(\tau_{v_4}-\tau_{v_2})}\right]\\ &+\left[\mathrm{e}^{\mathrm{i}\omega_{v_1}(\tau_{v_1}-\tau_{v_4})}-\mathrm{e}^{\mathrm{i}\omega_{v_1}(\tau_{v_4}-\tau_{v_1})}\right]\\ &\times\left.\left[\mathrm{e}^{\mathrm{i}\omega_{v_2}(\tau_{v_2}-\tau_{v_3})}-\mathrm{e}^{\mathrm{i}\omega_{v_2}(\tau_{v_3}-\tau_{v_2})}\right]\right\},\end{aligned}\tag{C.3}$$

$$\begin{aligned}\left\langle E_+^{\nu_4}(\tau_{v_4}, r_a)E_-^{\nu_1}(\tau_{v_1}, r_b)E_+^{\nu_2}(\tau_{v_2}, r_a)E_-^{\nu_3}(\tau_{v_3}, r_a)\right\rangle &= \int\frac{\mathrm{d}\omega_{v_3}}{2\pi}\mathcal{D}_{aa}^{(\nu,\nu')}(\omega_{v_3})\int\frac{\mathrm{d}\omega_{v_1}}{2\pi}\mathcal{D}_{ab}^{(\mu,\mu')}(\omega_{v_1})\\ &\times\left[\mathrm{e}^{\mathrm{i}\omega_{v_1}(\tau_{v_1}-\tau_{v_4})}-\mathrm{e}^{\mathrm{i}\omega_{v_1}(\tau_{v_4}-\tau_{v_1})}\right]\\ &\times\left[\mathrm{e}^{\mathrm{i}\omega_{v_3}(\tau_{v_2}-\tau_{v_3})}-\mathrm{e}^{\mathrm{i}\omega_{v_3}(\tau_{v_3}-\tau_{v_2})}\right],\end{aligned}\tag{C.4}$$

where $\mathcal{D}_{aa}^{(\nu,\nu')}(\omega)$ and $\mathcal{D}_{ab}^{(\nu,\nu')}(\omega)$ are given by equations (A.6), (A.5). Using the fact that $\mathcal{D}_{aa}^{(\nu,\nu')}(\omega)$ and $\mathcal{D}_{ab}^{(\nu,\nu')}(\omega)$ are odd functions the field correlation functions can be cast in the following form

$$\begin{aligned}\left\langle E_+^{\nu_4}(\tau_{v_4}, r_a)E_+^{\nu_3}(\tau_{v_3}, r_a)E_-^{\nu_2}(\tau_{v_2}, r_a)E_-^{\nu_1}(\tau_{v_1}, r_b)\right\rangle &= \int\frac{\mathrm{d}\omega_{v_1}}{2\pi}\mathcal{D}_{ab}^{(\nu,\nu')}(\omega_{v_1})\int\frac{\mathrm{d}\omega_{v_2}}{2\pi}\mathcal{D}_{aa}^{(\mu,\mu')}(\omega_{v_2})\\ &\times\left[\mathrm{e}^{\mathrm{i}\omega_{v_2}(\tau_{v_2}-\tau_{v_3})+\mathrm{i}\omega_{v_1}(\tau_{v_1}-\tau_{v_4})}\right.\\ &+\left.\mathrm{e}^{\mathrm{i}\omega_{v_2}(\tau_{v_2}-\tau_{v_4})+\mathrm{i}\omega_{v_1}(\tau_{v_1}-\tau_{v_3})}\right],\end{aligned}\tag{C.5}$$

$$\begin{aligned}\left\langle E_+^{\nu_4}(\tau_{v_4}, r_a)E_-^{\nu_3}(\tau_{v_3}, r_a)E_+^{\nu_2}(\tau_{v_2}, r_a)E_-^{\nu_1}(\tau_{v_1}, r_b)\right\rangle &= \int\frac{\mathrm{d}\omega_{v_1}}{2\pi}\mathcal{D}_{ab}^{(\nu,\nu')}(\omega_{v_1})\int\frac{\mathrm{d}\omega_{v_2}}{2\pi}\mathcal{D}_{aa}^{(\mu,\mu')}(\omega_{v_3})\\ &\times\mathrm{e}^{\mathrm{i}\omega_{v_3}(\tau_{v_3}-\tau_{v_4})+\mathrm{i}\omega_{v_1}(\tau_{v_1}-\tau_{v_2})},\end{aligned}\tag{C.6}$$

$$\begin{aligned}\left\langle E_+^{\nu_4}(\tau_{v_4}, r_a)E_+^{\nu_3}(\tau_{v_3}, r_a)E_-^{\nu_1}(\tau_{v_1}, r_b)E_-^{\nu_2}(\tau_{v_2}, r_a)\right\rangle &= \int\frac{\mathrm{d}\omega_{v_2}}{2\pi}\mathcal{D}_{aa}^{(\nu,\nu')}(\omega_{v_2})\int\frac{\mathrm{d}\omega_{v_1}}{2\pi}\mathcal{D}_{ab}^{(\mu,\mu')}(\omega_{v_1})\\ &\times\left[\mathrm{e}^{\mathrm{i}\omega_{v_1}(\tau_{v_1}-\tau_{v_3})+\mathrm{i}\omega_{v_2}(\tau_{v_2}-\tau_{v_4})}\right.\\ &+\left.\mathrm{e}^{\mathrm{i}\omega_{v_1}(\tau_{v_1}-\tau_{v_4})+\mathrm{i}\omega_{v_2}(\tau_{v_2}-\tau_{v_3})}\right],\end{aligned}\tag{C.7}$$

$$\begin{aligned}\left\langle E_+^{\nu_4}(\tau_{v_4}, r_a)E_-^{\nu_1}(\tau_{v_1}, r_b)E_+^{\nu_2}(\tau_{v_2}, r_a)E_-^{\nu_3}(\tau_{v_3}, r_a)\right\rangle &= \int\frac{\mathrm{d}\omega_{v_3}}{2\pi}\mathcal{D}_{aa}^{(\nu,\nu')}(\omega_{v_3})\int\frac{\mathrm{d}\omega_{v_1}}{2\pi}\mathcal{D}_{ab}^{(\mu,\mu')}(\omega_{v_1})\\ &\times\mathrm{e}^{\mathrm{i}\omega_{v_1}(\tau_{v_1}-\tau_{v_4})+\mathrm{i}\omega_{v_3}(\tau_{v_2}-\tau_{v_3})}.\end{aligned}\tag{C.8}$$

The integration over ω can be done using the identity

$$\int\mathrm{d}\omega_{v_1}\,\sin\left(\frac{\omega_v r_{ab}}{c}\right)\mathrm{e}^{\mathrm{i}\omega(\tau_1-\tau_2)}$$

$$= -\frac{2\pi}{\mathrm{i}}\left[\delta\left(\tau_1 - \tau_2 + \frac{r_{ab}}{c}\right) - \delta\left(\tau_1 - \tau_2 - \frac{r_{ab}}{c}\right)\right]. \tag{C.9}$$

The integration over ω_{v_2} can be using the identity

$$\int \mathrm{d}\omega_{v_3} \mathcal{D}_{aa}^{(\mu,\mu')}(\omega_{v_3}) \mathrm{e}^{\mathrm{i}\omega_{v3}(\tau_{v3}-\tau_{v4})}$$

$$= \frac{\hbar}{4\pi\epsilon_0 c^3}\left(\frac{\mathrm{i}}{2\pi}\right)^3 \delta_{\mu\mu'}\delta^{'''}(\tau_{v_3} - \tau_{v_4}), \tag{C.10}$$

where $\delta^{'''}$ is the third derivative of the delta-function. Inserting equations (C.9) and (C.10) into the field correlation equations (C.1)–(C.8) functions gives

$$\left\langle E_+^{\nu_4}(\tau_{v_4}, r_a) E_+^{\nu_3}(\tau_{v_3}, r_a) E_-^{\nu_2}(\tau_{v_2}, r_a) E_-^{\nu_1}(\tau_{v_1}, r_b)\right\rangle$$
$$= -\frac{\hbar}{2\pi\epsilon_0}\frac{\hbar}{4\pi\epsilon_0 c^3}\left(\frac{\mathrm{i}}{2\pi}\right)^3 \delta_{\mu\mu'}\left(-\nabla^2_{\nu\nu'} + \nabla_\nu \nabla_{\nu'}\right)$$
$$\times \frac{1}{r_{ab}}\left\{\delta^{'''}(\tau_{v_2} - \tau_{v_3})\left[\delta\left(\tau_{v_1} - \tau_{v_4} + \frac{r_{ab}}{c}\right) - \delta\left(\tau_{v_1} - \tau_{v_4} - \frac{r_{ab}}{c}\right)\right] + \delta^{'''}(\tau_{v_2} - \tau_{v_4})\left[\delta\left(\tau_{v_1} - \tau_{v_3} + \frac{r_{ab}}{c}\right) - \delta\left(\tau_{v_1} - \tau_{v_3} - \frac{r_{ab}}{c}\right)\right]\right\}, \tag{C.11}$$

$$\left\langle E_+^{\nu_4}(\tau_{v_4}, r_a) E_-^{\nu_3}(\tau_{v_3}, r_a) E_+^{\nu_2}(\tau_{v_2}, r_a) E_-^{\nu_1}(\tau_{v_1}, r_b)\right\rangle$$
$$= -\frac{\hbar}{2\pi\epsilon_0}\frac{\hbar}{4\pi\epsilon_0 c^3}\left(\frac{\mathrm{i}}{2\pi}\right)^3 \delta_{\mu\mu'}\left(-\nabla^2_{\nu\nu'} + \nabla_\nu \nabla_{\nu'}\right)$$
$$\times \frac{1}{r_{ab}}\left\{\delta^{'''}(\tau_{v_3} - \tau_{v_4})\left[\delta\left(\tau_{v_1} - \tau_{v_2} + \frac{r_{ab}}{c}\right) - \delta\left(\tau_{v_1} - \tau_{v_2} - \frac{r_{ab}}{c}\right)\right]\right\}, \tag{C.12}$$

$$\left\langle E_+^{\nu_4}(\tau_{v_4}, r_a) E_+^{\nu_3}(\tau_{v_3}, r_a) E_-^{\nu_1}(\tau_{v_1}, r_b) E_-^{\nu_2}(\tau_{v_2}, r_a)\right\rangle$$
$$= -\frac{\hbar}{2\pi\epsilon_0}\frac{\hbar}{4\pi\epsilon_0 c^3}\left(\frac{\mathrm{i}}{2\pi}\right)^3 \times \delta_{\mu\mu'}\left(-\nabla^2_{\nu\nu'} + \nabla_\nu \nabla_{\nu'}\right)$$
$$\times \frac{1}{r_{ab}}\left\{\left[\delta\left(\tau_{v_1} - \tau_{v_3} + \frac{r_{ab}}{c}\right) - \delta\left(\tau_{v_1} - \tau_{v_3} - \frac{r_{ab}}{c}\right)\right]\delta^{'''}(\tau_{v_2} - \tau_{v_4}) + \left[\delta\left(\tau_{v_1} - \tau_{v_4} + \frac{r_{ab}}{c}\right) - \delta\left(\tau_{v_1} - \tau_{v_4} - \frac{r_{ab}}{c}\right)\right]\delta^{'''}(\tau_{v_2} - \tau_{v_3})\right\}, \tag{C.13}$$

$$\left\langle E_+^{\nu_4}(\tau_{v_4}, r_a) E_-^{\nu_1}(\tau_{v_1}, r_b) E_+^{\nu_2}(\tau_{v_2}, r_a) E_-^{\nu_3}(\tau_{v_3}, r_a)\right\rangle$$
$$= -\frac{\hbar}{2\pi\epsilon_0}\frac{\hbar}{4\pi\epsilon_0 c^3}\left(\frac{\mathrm{i}}{2\pi}\right)^3 \delta_{\mu\mu'}\left(-\nabla^2_{\nu\nu'} + \nabla_\nu \nabla_{\nu'}\right)$$
$$\times \frac{1}{r_{ab}}\left[\delta\left(\tau_{v_1} - \tau_{v_4} + \frac{r_{ab}}{c}\right) - \delta\left(\tau_{v_1} - \tau_{v_4} - \frac{r_{ab}}{c}\right)\right]\delta^{'''}(\tau_{v_2} - \tau_{v_3})\Bigg\}. \tag{C.14}$$

References

[1] Bloembergen N 1965 *Nonlinear Optics: Lecture Note and Reprint Volume* (New York: Benjamin)

[2] Mukamel S 1995 *Principles of Nonlinear Optical Spectroscopy* (Oxford: Oxford University Press)

[3] Mukamel S 2003 Superoperator representation of nonlinear response: unifying quantum field and mode coupling theories *Phys. Rev.* E **68** 021111

[4] Tanimura Y and Mukamel S 1993 Two-dimensional femtosecond vibrational spectroscopy of liquids *J. Chem. Phys.* **99** 9496–511

[5] Fourkas J T, Kawashima H and Nelson K A 1995 Theory of nonlinear optical experiments with harmonic oscillators *J. Chem. Phys.* **103** 4393–407

[6] Hamm P, Helbing J and Bredenbeck J 2008 Two-dimensional infrared spectroscopy of photoswitchable peptides *Annu. Rev. Phys. Chem.* **59** 291–317

[7] Chung H S, Ganim Z, Jones K C and Tokmakoff A 2007 Transient 2D IR spectroscopy of ubiquitin unfolding dynamics *Proc. Natl Acad. Sci. USA* **104** 14237–42

[8] Fang C, Wang J, Kim Y S, Charnley A K, Barber-Armstrong W, Smith A B, Decatur S M and Hochstrasser R M 2004 Two-dimensional infrared spectroscopy of isotopomers of an alanine rich α-helix *J. Phys. Chem.* B **108** 10415–27

[9] Eaves J D, Loparo J J, Fecko C J, Roberts S T, Tokmakoff A and Geissler P L 2005 Hydrogen bonds in liquid water are broken only fleetingly *Proc. Natl Acad. Sci.* **102** 13019–22

[10] Khalil M, Demirdven N and Tokmakoff A 2003 Obtaining absorptive line shapes in two-dimensional infrared vibrational correlation spectra *Phys. Rev. Lett.* **90** 047401

[11] Zheng J, Kwak K, Asbury J, Chen X, Piletic I R and Fayer M D 2005 Ultrafast dynamics of solute–solvent complexation observed at thermal equilibrium in real time *Science* **309** 1338–43

[12] Germeau A, Roest A L, Vanmaekelbergh D, Allan G, Delerue C and Meulenkamp E A 2003 Optical transitions in artificial few-electron atoms strongly confined inside zno nanocrystals *Phys. Rev. Lett.* **90** 097401

[13] Cundiff S T, Zhang T, Bristow A D, Karaiskaj D and Dai X 2009 Optical two-dimensional fourier transform spectroscopy of semiconductor quantum wells *Acc. Chem. Res.* **42** 1423–32

[14] Kovalevskij V, Gulbinas V, Piskarskas A, Hines M A and Scholes G D 2004 Surface passivation in CdSe nanocrystalpolymer films revealed by ultrafast excitation relaxation dynamics *Phys. Stat. Sol.* **241** 1986–93

[15] Dai X, Richter M, Li H, Bristow A D, Falvo C, Mukamel S and Cundiff S T 2012 Two-dimensional double-quantum spectra reveal collective resonances in an atomic vapor *Phys. Rev. Lett.* **108** 193201

[16] Glinka Y D, Erementchouk M, Dass C K, Leuenberger M N, Bracker A S and Li X 2013 Non-local coherent coupling between excitons in a disordered quantum well *New J. Phys.* **15** 075026
[17] Doust A B, van Stokkum I H M, Larsen D S, Wilk K E, Curmi P M G, van Grondelle R and Scholes G D 2005 Mediation of ultrafast light-harvesting by a central dimer in phycoerythrin 545 studied by transient absorption and global analysis *J. Phys. Chem.* B **109** 14219–26
[18] Abramavicius D, Palmieri B, Voronine D V, Sanda F and Mukamel S 2009 Coherent multidimensional optical spectroscopy of excitons in molecular aggregates; quasiparticle versus supermolecule perspectives *Chem. Rev.* **109** 2350–408
[19] Agarwal D G S 1974 *Quantum Statistical Theories of Spontaneous Emission and Their Relation to Other Approaches* (Berlin: Springer)
[20] Andrews D L 1997 *Lasers in Chemistry* (Berlin: Springer)
[21] Bennett K and Mukamel S 2014 Cascading and local-field effects in nonlinear optics revisited: a quantum-field picture based on exchange of photons *J. Chem. Phys.* **140** 044313
[22] Dorfman K E and Mukamel S 2013 Collective resonances in $\chi^{(3)}$: a qed study *Phys. Rev.* A **87** 063831
[23] Harbola U and Mukamel S 2008 Superoperator nonequilibrium Green's function theory of many-body systems; applications to charge transfer and transport in open junctions *Phys. Rep.* **465** 191–222
[24] Scully M O 1997 *Quantum Optics: XD-US.* (Cambridge: Cambridge University Press)
[25] Konar A, Shah J D, Lozovoy V V and Dantus M 2012 Optical response of fluorescent molecules studied by synthetic femtosecond laser pulses *J. Phys. Chem. Lett.* 1329–35
[26] Konar A, Lozovoy V V and Dantus M 2012 Solvation stokes-shift dynamics studied by chirped femtosecond laser pulses *J. Phys. Chem. Lett.* **17** 2458–64
[27] Salam A 2010 *Molecular Quantum Electrodynamics: Long-Range Intermolecular Interactions* (New York: Wiley)